Inflammatory effects in zebrafish (*Danio rerio*) exposed to gold nanoparticles

Eline Skadberg

Master's Thesis in Toxicology

Department of Biosciences
The Faculty of Mathematics and Natural Sciences

UNIVERSITY OF OLSO
June 2015

Acknowledgements

The work presented in this thesis was conducted at the Department of Production Animal Clinical Science (ProdMed) at the Norwegian University of Life Sciences (NMBU) for the Master's degree in Toxicology at the University of Oslo (UiO). This thesis was a part of the NanEAU (II) project "Environmental health risk evaluation for nanostructures developed for water remediation", in collaboration and financially supported by the Luxembourg Institute of Science and Technology (LIST).

First, I would like to thank my supervisors at NMBU, Professor Erik Ropstad and associate researcher Karin Zimmer, for the opportunity, help with statistics and constructive comments. Thank you to my supervisor Professor Ketil Hylland at UiO for giving me a solid background in toxicology, and to Dr. Arno Gutleb and partners at LIST for the nanoparticles and the NTA. I would especially like to thank my co-supervisor PhD candidate Julia Tandberg at the Department of Pharmaceutical Biosciences, UiO, not only for teaching me all of the methods, but for good advice, quick replies and guidance.

In addition, I would like to express my gratitude to the facilities manager at the Model Fish Unit, Ana Sulen Tavara for good spirits and for teaching me everything I know about the amazing zebrafish, to Dr. Thomas Fraser, NMBU, for always answering my questions and giving detailed comments, and to Federico Fenaroli at EM lab at UiO for imaging of the nanoparticles.

A special thanks to my fellow master student German Herranz for coffee breaks, discussions, more coffee, and for a good time at NMBU. Thank you to my friends and family for good support, and last, but definitely not least, to Andreas for your encouragement, patience and for keeping me sane.

Oslo, June 2015
Eline Supannee Setu Skadberg

Abstract

Due to their unique physical and chemical properties, gold nanoparticles (AuNPs) are promising in a wide variety of biomedical applications. However, there are several indications that AuNPs may be toxic and that particle size is an important factor. The immune system plays a key role in the biological response to nanoparticles and inflammation has been commonly associated with nanoparticle induced toxicity. The main objective of this study was therefore to investigate the inflammatory potential of three different sizes of AuNPs, *in vivo*, using the zebrafish embryo model.

Briefly, zebrafish embryos were injected intravascularly with sub-lethal doses (0.1, 0.5 or 1.0 μg/mL) of 20, 40 or 80 nm citrate stabilized AuNPs at 72h post fertilization (hpf). Three replicates of the injected and the control fish were collected at 2, 24 and 48 h post injection (hpi) and the expression of proinflammatory (*tnfa, il1b, il8, il12a* and *ifng*) and anti-inflammatory (*il10*) genes related to the innate immune system were measured by reverse transcription-quantitative PCR (RT-qPCR). Survival studies in zebrafish were conducted prior to the immune response assessment to determine a sub-lethal dose range, and revealed only moderate effects on survival following exposure to 80 nm AuNPs.

Results from the gene expression analysis showed an increased transcription of all the inflammatory genes, primarily at 2 hpi, which subsided to control levels by 48 hpi. The transcription of the proinflammatory cytokines TNF-α, IL-1β and IFNγ was considerably lower for 20 nm AuNPs and might reflect differences related to particle size. The observed effects did not seem to be highly correlated with the injected dose, although there was a tendency for the highest doses to elicit the highest response. Overall, this study suggests that the examined AuNPs induce a transient, inflammatory response in zebrafish.

Table of contents

Acknowledgements I

Abstract III

Abbreviations VII

1. INTRODUCTION 1

1.1. Nanoparticles 1

1.2 Gold nanoparticles 2
1.2.1 Synthesis, Size distribution and characterization of gold nanoparticles 3
1.2.2 Distribution of nanoparticles 4
1.2.3 Inflammation 6
1.2.4 Toxicity of gold nanoparticles 7

1.4 The zebrafish (Danio rerio) as a model organism 9
1.4.1 Zebrafish as a model for toxicology 10

1.5 Project objectives 12

2. MATERIALS AND METHODS 13

2.1 Gold nanoparticles 13
2.1.2 Characterization of gold nanoparticles 13

2.2 Zebrafish maintenance and breeding 14

2.3 Microinjection in zebrafish 15

2.4 Survival assessment 16

2.5 Immune response 17
2.5.1 Microinjection of gold nanoparticles 17
2.5.2 Sampling of material for gene expression analysis 18
2.5.3 Extraction of total RNA 19
2.5.4 Reverse transcription: cDNA synthesis 20
2.5.5 Primers and quantitative PCR 21

2.6 Statistical analysis 23

3. RESULTS 25

3.1 Characterization of gold nanoparticles 25

3.2 Survival assessment 27

3.3 Expression of inflammatory genes 28

4. DISCUSSION **34**

4.1 Characterization **34**

4.2 Zebrafish embryo survival **35**

4.3 Expression of inflammatory genes **36**
4.3.1 Methodical considerations 38

5. CONCLUSION **40**

FUTURE PERSPECTIVES **41**

References **42**
Appendix A: Kit protocols 54
Appendix B: Pilot study and other results 57

Abbreviations

AAALAC	The Association for Assessment and Accreditation of Laboratory Animal Care International
AuNPs	Gold nanoparticles
cDNA	Complementary DNA
dH_2O	Distilled water
C_t	Cycle threshold
dpf	Days post fertilization
DLS	Dynamic light scattering
DNase	Deoxyribonuclease
ENPs	Engineered nanoparticles
FET	Fish embryo acute toxicity test
hpf	Hours post fertilization
hpi	Hours post injection
IFNγ	Interferon gamma
IL	Interleukin
LIST	Luxembourg Institute of Science and Technology
MFlab	Model fish laboratory
N_F	Normalization factor
NIR	Near infrared
NMBU	The Norwegian University of Life Sciences
NPs	Nanoparticles
NTA	Nanoparticle tracking analysis

OECD	Organisation for Economic Co-operation and Development
PBS	Phosphate buffered saline
PEG	Polyethylene glycol
RME	Receptor mediated endocytosis
ROS	Reactive oxygen species
RT	Reverse transcription
qPCR	Quantitative polymerase chain reaction
TEM	Transmission electron microscopy
TNF-α	Tumor necrosis factor alpha
ZFET	Zebrafish embryo acute toxicity test
β-ME	2- Mercaptoethanol

1. Introduction

1.1. Nanoparticles

Nanoparticles (NPs) are defined as structures with one or more dimensions less than 100 nm. With decreasing particle size, there is an exponential increase in the surface area relative to the volume. The increased surface area may affect the chemical reactivity and impart unique features to NPs, such as increased strength and electrical conductivity when compared to materials on the macroscopic scale (Hornyak et al., 2009). These unique properties make NPs highly attractive in nanotechnology, which involves the deliberate synthesis and manipulation of nanoparticles (Kessler 2011).

The potential diversity of engineered nanoparticles (ENPs), each with distinct properties is enormous when considering the possible variations in shape, size and chemical composition and it is becoming increasingly apparent that nanotechnology holds great promise for novel applications, especially within biomedicine, electronics and material science (Roco et al., 2005a; Piccinno et al., 2012). However, the same characteristics that make ENPs so promising may also influence their behavior in a biological system (Donaldson et al., 2004; Oberdorster et al., 2005a). This has raised concerns about the safety of NPs, as their nanoscale dimensions may lead to toxic properties that differ from bulk-sized material of the same composition (Oberdorster et al., 2005b).

Despite the increased production volume and use of NPs, knowledge about their adverse health effects is relatively limited (Roco 2005b). Importantly, several nanomaterials are being evaluated for medical use, such gold nanoparticles in targeted drug delivery systems (Hurst 2011). The medical applications of NPs represents a modern entry route for NPs (Aillon et al., 2009), and the potential toxicity following intentional exposure should be examined.

1.2 Gold nanoparticles

Gold is a noble, metallic element and is by nature highly inert. In bulk, gold is generally considered non-toxic and historically, gold based compounds have been used to treat infectious diseases such as tuberculosis and have been used therapeutically to treat rheumatoid arthritis (Sigler et al., 1974; Benedek 2004). More recently, due to their high stability and the ease to which surface properties (e.g. surface functional groups) can be manipulated (Kamat 2002), gold nanoparticles (AuNPs) have become the focus of an extensive amount of biomedical research (Hirsch et al., 2003; Huang et al., 2006; Kirpotin et al., 2006).

On the nanoscale, the properties of gold are highly influenced by their size and shape (Bhattacharya et al., 2008). Of particular interest is that a relatively narrow frequency of light can induce oscillations in the de-localized surface electrons (i.e. surface plasmons) of AuNPs (Daniel et al., 2004). This phenomenon is called the localized surface plasmon resonance (LSPR), which for AuNPs occurs in the visible and near-infrared region (NIR) of the electromagnetic spectrum. For spherical AuNPs a single plasmon band is observed in the visible region and can readily be observed with gold colloids; as the particle size increases, the absorption shifts to longer wavelengths (Kelly et al., 2003) and smaller particles (5-20 nm) may appear red in color, while larger particles (80-100 nm) can appear purple and brown.

These optical properties can be “fine-tuned” by modifying the size and the shape, and constitutes the basis for the biomedical applications of gold nanoparticles (Lee et al., 2006). For example, in targeted photothermal therapy, rod–shaped, injectable gold nanoparticles are being designed to absorb specific wavelengths in the NIR region. The exited surface electrons in the conduction band lose their energy in the form of heat, at temperatures that are sufficient to destroy nearby cells (e.g. cancerous cells) (Huang et al., 2006). Other biomedical applications of AuNPs include targeted delivery systems, diagnostics and medical imaging (Hurst 2011).

1.2.1 Synthesis, Size distribution and characterization of gold nanoparticles

Currently, most methods used to synthesize gold nanoparticles follow a similar strategy. In these methods dissolved gold salts are reduced in the presence of surface capping agents to stabilize the particles and prevent aggregation by electrostatic or physical repulsion (Dreaden et al., 2012). The particle size can be controlled by adjusting the ratio of gold ions and the reducing agent (Khan et al., 2013). The refined Turkevich method (Turkevich et al., 1951; Frens 1973) is the simplest and most common method used to synthesize gold nanoparticles (Daniel et al., 2004). In this method, chlorauric acid ($HAuCl_4$) is reduced in an aqueous solution by utilizing sodium citrate as both the reducing and - capping agent. In general, smaller amounts of citrate will result in larger particles. This method is known to produce spherical, monodisperse gold nanoparticles (gold colloids) in the size range of 9-120 nm (Kimling et al., 2006).

Producing AuNPs leads to unique properties that are not found in the bulk material, however these benefits may be lost if the particles aggregate. Colloidal stability is known to be highly dependent on particle surface charge and environmental conditions such as pH, temperature and ionic strength (Fubini et al., 2010), and when introduced into a new test system AuNPs have been shown to form agglomerates (Dobrovolskaia et al., 2009; Wang et al., 2010). Agglomeration may shift the size distribution towards larger sizes and alter the physicochemical properties (i.e. size and surface area) of NPs, which can have important implications for their distribution as well as their toxicological properties (Albanese et al., 2011).

Because the shape, size and the state of agglomeration are important in determining the biological fate of nanoparticles, it is recommended that nanoparticles be characterized prior to exposure (Powers et al., 2007). Since gold is electron-dense, it is easy to identify AuNPs using transmission electron microscopy (TEM). TEM generates highly resolved images and is commonly used to gain information about the size distribution and

morphology of a sample. However, sample preparation for TEM imaging often involves drying, which may result in agglomeration of the sample (Bohnsack et al., 2012). Microscopy methods for characterization should therefore be coupled with other methods to characterize the particles in the relevant media. Dynamic light scattering (DLS) methods are commonly used in nanotoxicological studies and are useful to evaluate the aggregation status (Murdock et al., 2008). However, the presence of larger particles may highly influence the intensity of the light scattered and may distort the average particle size towards larger sizes (Filipe et al., 2010).

Nanoparticle tracking analysis (NTA) is a more recently developed method that may also provide information about the aggregation in a sample (Du et al., 2012). The NTA method utilizes the properties of both light scattering and random Brownian movements to characterize the hydrodynamic diameter of the particles in a liquid suspension. Further, the NTA technique follows individual particles, rather than averaging over a sample, and has been shown to accurately analyze the size distribution of particle suspensions (Filipe et al., 2010).

1.2.2 Distribution of nanoparticles

Many of the applications of AuNPs will eventually result in particles being introduced into a biological system (Alkilany et al., 2010), and direct exposure is a regarded as a likely route of exposure for AuNPs in humans (Aillon et al., 2009).

Due to their small size, nanoparticles have been shown to gain access to several biological compartments that are usually protected from larger particles (Oberdorster et al., 2005a; Fubini et al., 2010). For instance, nasally administered titanium dioxide (TiO_2) NPs were found to directly enter the brain through the olfactory bulb in mice (Wang et al., 2008), which has not been observed for bulk-sized TiO_2 (Oberdorster et al., 2005a). The exposure was associated with significant oxidative damage and inflammation in the brain, which raises concerns about the potential neurotoxicity of NPs.

Several animal studies have demonstrated the ability of AuNPs to redistribute to various organs, such as the liver, spleen, lung, heart and brain, following oral administration and various routes of injection (Hillyer et al., 2001; De Jong et al., 2008; Khan et al., 2013). In the bloodstream, NPs have been shown to interact with plasma proteins, which may have a substantial effect on their cellular uptake, clearance and toxicity (Dobrovolskaia et al., 2009; Simpson et al., 2010; Lee et al., 2015). Again, nanoparticle characteristics such as size, shape, surface charge and agglomeration are among the contributing factors determining the interactions with proteins (Monopoli et al., 2011)

The cellular uptake up AuNPs has been found to be highly dependent on size and shape (Goodman et al., 2004; De Jong et al., 2008; Chen et al., 2009). Chithrani et al., (2006) examined the cellular uptake of a wide size range of citrate stabilized AuNPs in HeLa cells. It was determined that endocytosis was most efficient for the medium-sized, 50 nm spheres compared to 14 and 74 nm AuNPs. Further, it was shown that the cellular uptake of AuNPs was dependent on particle shape, with sphere-shaped particles being much more efficiently taken up than their rod-shaped counterparts. For both shapes, the mechanism of cellular entry was determined to be receptor mediated endocytosis (RME), through the adsorption of non-specific serum proteins.

For purposes of medical applications, AuNPs may be functionalized with surface coatings to alter their behavior within a biological system. For example, the adsorption of opsonins, proteins that make foreign material visible to phagocytic cells of the immune system (Walkey et al., 2012), has been shown to highly influence the biological fate of NPs (Dobrovolskaia et al., 2009). This is because following opsonization, phagocytosis can occur, which may lead to the eventual degradation or removal of particles from the bloodstream (Owens et al., 2006). For biomedical applications, this is generally an undesired effect and highlights the role of the immune system in removing NPs from the host by facilitating excretion through the liver and spleen (Storm et al., 1995; Alexis et al., 2008). For these reasons, several AuNPs for biomedical use are being synthesized with various surface functional groups such as polyethylene glycol (PEG), to prolong systemic circulation and to avoid interaction with the immune system (Paciotti et al., 2004).

Although the immune cells play an important role in removing them from the body, NPs are also taken up by cells from other systems. For example, inhaled TiO2 NPs have been shown to accumulate in erythrocytes, which lack phagocytic receptors. In this case, cellular uptake was entirely dependent on particle size (Geiser et al., 2005). The internalization of nanoparticles have been shown to occur through several different pathways (Kettiger et al., 2013), including pinocytosis (Shukla et al., 2005) and RME (Chithrani et al., 2006). Intracellularly, NPs have been shown to localize in cellular compartments, such as the cytosol, lysosomes, endosomes, mitochondria and the nucleus (Berry et al., 2007; AshaRani et al., 2009; Kim et al., 2009; Li et al., 2010; Schaeublin et al., 2011), although the various uptake mechanisms are unclear.

1.2.3 Inflammation

There is increasing evidence that NPs, due to their increased surface reactivity, induce toxicity through the generation of reactive oxygen species (ROS) (Hussain et al., 2005; Karlsson et al., 2008; Xia et al., 2008; Pan et al., 2009). In excess, the generation of ROS can cause severe damage to cellular components through the oxidation of lipids, proteins and DNA and may cause toxicity through the induction of oxidative stress and inflammation (Klaasen 2001).

Nanoparticles have been reported to induce ROS production in several different ways. For instance, carbon nanotubes have been shown to generate ROS directly due to oxidants on the particle surface (He et al., 2011) and AuNPs have been shown to generate ROS through the internalization and activation of phagocytic cells in the immune system (Bastus et al., 2009; Sharma et al., 2013). The innate immune system represents the first line of defense in an organism (Mogensen 2009)and has therefore, not surprisingly, been suggested to play a key role in the biological response to nanoparticles (Oberdorster et al., 2005a). The nanoparticle induced ROS generation may trigger an immune response through the activation of redox sensitive mitogen-activated protein kinases (MAPK) and nuclear factor

kappa B (NF-kB) signaling pathways, which are highly involved in regulating the production of inflammatory cytokines (Thannickal et al., 2000; Buzea et al., 2007).

Inflammatory cytokines are signaling proteins that primarily are secreted by activated immune cells, such as macrophages and neutrophils. Examples are interleukins (IL), interferons (IFN) and tumor necrosis factors (TNF). Their main function is to regulate the magnitude of the immune response through the balance between proinflammatory cytokines, such as TNF-α, IL-1β, IFNγ, and anti-inflammatory cytokines, such as IL-10 (Opal et al., 2000; Commins et al., 2010). Inflammation normally promotes healing and is a temporary response to injury and infection. However, if not regulated correctly or disturbed by a toxic insult, an acute inflammation can in itself cause damage through the action of the inflammatory mediators TNF-α and IL-1β which are involved in apoptosis, cell proliferation and tissue destruction (Balkwill et al., 2001). Alternatively, the inflammation may be driven into a chronic state in which surrounding cells and tissues are continuously injured (Licastro et al., 2005). In a human health perspective, inflammation has been linked to major diseases such as Alzheimer's, diabetes and cancer (Balkwill et al., 2001). Because cytokines modulate the immune response, they are generally considered as biomarkers for immunotoxicity (Elsabahy et al., 2013) and the inflammatory potential of NPs can be assessed by measuring transcriptional changes of proinflammatory genes (Yen et al., 2009).

1.2.4 Toxicity of gold nanoparticles

In vitro studies have suggested that the potential toxicity of AuNPs is related to factors such as size, surface charge and shape (Khlebtsov et al., 2011). For instance, Pan et al., (2009) investigated the cytotoxic effect of a wide size range of spherical AuNPs (0.8 – 15 nm) in several mammalian cell lines. It was found that the 1.4 nm AuNPs triggered necrosis and oxidative stress in all the investigated cell lines, whereas 1.2 nm AuNPs induced cellular death through apoptotic mechanisms. No cellular damage was observed for 15 nm AuNPs, even at the highest concentrations, suggesting a size-dependent toxicity

of gold nanoparticles. In addition to size, the surface charge has been shown to influence cellular toxicity (Schaeublin et al., 2011; Liu et al., 2013). Cationic AuNPs have been shown to display moderate toxicity in COS-1 cells *and E. Coli,* whereas anionic AuNPs displayed no toxicity, perhaps due to interactions with the negatively charged cell membrane (Goodman et al., 2004). However, some studies have demonstrated the biocompatibility of AuNPs and suggest that they are not cytotoxic. In fact, AuNPs have been demonstrated to have an antioxidant effect in RAW264.7 macrophages (Shukla et al., 2005).

The *in vivo* distribution and toxicity of AuNPs has been shown to be size-dependent in rodents following various routes of injection and oral administration (Hillyer et al., 2001; De Jong et al., 2008) and the liver has been shown to be an important site of accumulation. For example, the results of De Jong et al. (2008) demonstrated that the smallest particle size tested (10 nm), had the widest tissue distribution (blood, liver, spleen, kidney, testis, thymus, lung and brain) with the highest accumulation of AuNPs observed in the liver and spleen of rats. Further, Cho at al., (2009) found that 13 nm PEG coated AuNPs accumulated in the liver of mice following intravenous injection, where AuNPs was associated with apoptosis and acute liver inflammation. The observed toxicity was associated with a dose-dependent and transient increase of proinflammatory cytokines (TNF-α, IL-1β). Similar results were found by Kahn et al., (2013) in rats exposed to 10 and 50 nm AuNPs. Here, it was reported that the 50 nm particles induced the most severe inflammation in the liver, as measured by liver pathology and the increase of proinflammatory cytokines (TNF-α, IL-β and IL-6).

Several studies have examined the toxicity of AuNPs in zebrafish (*Danio rerio*), which are proving to be a robust vertebrate model for assessing nanotoxicity (Fako et al., 2009). In zebrafish, AuNPs have been reported to be moderately toxic when compared to NPs composed of elements with higher toxicity, such as silver and copper (Bar-Ilan et al., 2009; Asharani et al., 2011; Kovriznych et al., 2013). Others have suggested that AuNPs are toxic to zebrafish and have reported embryonic lethality, developmental toxicity (Truong et al., 2012) and neurotoxicity (Kim et al., 2013). In the mentioned studies, the toxicity of the examined AuNPs was highly dependent on the surface charge, with cationic AuNPs being

most toxic, Further, the exposure to the charged AuNPs was found to have significant effects in the regulation of genes related to the immune system and inflammation (Truong et al., 2012).

1.4 The zebrafish (*Danio rerio*) as a model organism

The zebrafish, *Danio rerio* (Hamilton 1822), is a small fresh water fish in the minnow family (*Cyprinidae*). They are native to the tropical waters of North-Eastern India and Bangladesh, where they are abundant and are commonly found in slow moving streams adjacent to rice fields (Engeszer et al., 2007).

The zebrafish has been used for several decades as a vertebrate model for developmental biology and molecular genetics (Driever et al., 1996; Haffter et al., 1996). The small size, high fecundity and short generation time allows for rapid evaluation of the toxicity of a large amount of compounds (Taylor et al., 2010). Compared to other vertebrate models, zebrafish are relatively easy to maintain and are cost efficient with regards to husbandry, housing and use of chemicals. Newly fertilized embryos are approximately 1 mm in diameter and in captivity, adult zebrafish rarely exceed 5 -6 cm. Sexual maturity reaches a maximum at 7-18 months of age and under optimal conditions a single pair of zebrafish can produce 200-300 embryos each week (Westerfield 2000).

Zebrafish embryonic development is rapid; hatching from the chorion occurs at 42-72 hours post fertilization (hpf) and the majority of morphogenesis and organogenesis is completed by 120 hpf (Kimmel et al., 1995). Furthermore, development takes place *ex-utero* and embryos maintain a high degree optical transparency throughout development and early larval stages. These features, coupled with the well-described developmental stages of zebrafish (Kimmel et al., 1990) enables easy administration of compounds and more importantly, the real-time assessment of biological responses. In addition, the zebrafish genome has been fully sequenced by the Wellcome Trust Sanger Institute (Hinxton, UK) and appears to be highly homogenous to that of humans (Howe et al., 2013).

The zebrafish model system offers several advantages in immunological research: they are one of the smallest vertebrate models to possess a fully functional innate and adaptive immune system, the immune system in zebrafish is highly conserved when compared to mammals (Trede et al., 2004; Stein et al., 2007) and there are many molecular tools and transgenic lines available to examine interactions and responses of cells in the immune system (Brudal et al., 2014). The transparency of the embryos has allowed for studies of the immune system at earlier points in development (Yoder, 2002) and macrophages and neutrophils of the innate immune system can be observed as early as 23 hpf and are fully functional by 48 hpf (Herbomel et al., 1999). While the innate immune system is present early in development, the adaptive immune system is not fully developed in zebrafish until 3-4 weeks post fertilization (Lam et al., 2004) This separation allows for isolated studies of the innate immune system, independently from the adaptive immune system (Traver et al., 2003).

1.4.1 Zebrafish as a model for toxicology

More recently, the zebrafish has emerged as an attractive model in toxicology for screening of chemicals (Zhang et al., 2003; Zon et al., 2005; Sipes et al., 2011), and nanoparticles (Fako et al., 2009). The zebrafish has been shown to exhibit similar physiological responses to xenobiotics as mammals (Rubinstein 2006) and have been especially useful in toxicology to screen for developmental toxicants (Selderslaghs et al., 2009) and environmental pollutants, such as pesticides and heavy metals (King-Heiden et al., 2012; Jin et al., 2015).

There is currently a commitment in the European regulatory framework towards the development of alternative models in risk assessment and scientific research (Braunbeck et al., 2014). Because zebrafish do not feed externally until 120 hpf (Westerfield 2000), they are not subject to the European commission (EC) directive 86/609/EEC, which regulates the use of animals in scientific experiments and are, as such considered as an alternative model. The zebrafish embryo acute toxicity test (ZFET, OECD TG 236) was recently made

available by the Organisation for Economic Co-operation and Development (OECD), as an alternative to the fish embryo toxicity test (FET, OECD TG 203), as an attempt to replace and reduce the use of juvenile and adult fish in risk assessment (Busquet et al., 2014).

The use of the ZFET test for (eco)nanotoxicological studies is promising, when considering the diversity of nanomaterials being produced and the high-throughput screening potential of zebrafish (Piccinno et al., 2012; Clemente et al., 2014). Most nanotoxicological studies in zebrafish have been performed using waterborne exposure in embryos, which more closely resembles natural conditions and is the recommended route of exposure in the ZFET test. Dietary exposure is also relevant for NPs, as they may accumulate in food chains (Croteau et al., 2011) and has been examined in zebrafish (Park et al., 2010; Geffroy et al., 2012). Only a few studies have used microinjection as the primary exposure route (Harper et al., 2008; Cheng et al., 2009), which is a useful method to precisely deliver a specific amount of NPs to distinct anatomical sites. Microinjection may not reflect natural exposure, but can be used to efficiently bypass biological barriers such as the chorion or the skin, which is relevant for the biomedical applications of NPs (Bohnsack et al., 2012).

1.5 Project objectives

Due to size related properties, gold nanoparticles are highly promising in a variety of biomedical applications. However, nanoparticles are suggested to induce toxicity trough mechanisms associated with inflammation and nanotoxicological studies are as such, becoming increasingly relevant. Recently, the zebrafish have emerged as an important model organism for evaluating the toxicity of nanoparticles. The main objective of this study was therefore to investigate the inflammatory potential of AuNPs using the zebrafish as a model system.

We hypothesized that AuNPs of three different sizes would induce an inflammatory response in zebrafish embryos, and that the level of this response would be positively associated with the dose and the particle size. To test this this hypothesis, zebrafish were exposed to sub-lethal doses of 20, 40 and 80 nm AuNPs through intravascular injection and the transcription of inflammatory cytokines were measured at 2, 24 and 48 hours post injection. AuNPs were characterized prior to exposure and survival assessments in zebrafish were performed to determine a sub-lethal dose range.

2. Materials and methods

2.1 Gold nanoparticles

Citrate stabilized gold nanoparticles were purchased commercially at nanoComposix Europe (NanoXact ™, Prague, Czech Republic) and were kindly donated to the project by Dr. Arno Gutleb from the Luxembourg Institute of Science and Technology (LIST). Stock solutions of 20, 40 and 80 nm spherical gold nanoparticles (gold colloid, CAS-no: 7440-57-5) were received as a 1 mg/ml suspension dissolved in a sodium citrate buffer (>99 % water). The mean diameter of the gold nanoparticles (AuNPs) was specified by the manufacturer to be 20 ±3 nm, 40±4 nm and 80±5 nm. The received AuNPs were kept at 4°C and away from light for long-term storage until required. For simplicity, the manufacturer specified sizes have been used throughout this thesis.

2.1.2 Characterization of gold nanoparticles

Transmission electron microscopy (TEM) (CM100, Phillips, Amsterdam, Netherlands) and imaging (Quemesa, Olympus, Tokyo, Japan) was used to characterize the morphology and the size distribution of the AuNPs. TEM was performed following established procedures at the electron microscopy laboratory at the Department of Biosciences at The University of Oslo (UiO). Prior to TEM, the AuNPs were allowed to adsorb to carbon coated formvar copper grids. The grids for electron microscopy were briefly placed on one droplet (~20 µl) of the AuNP stock solutions and were gently removed after approximately one minute. Excess fluid was removed by gently blotting with filter paper and the grids were left to dry for 1-2 minutes before imaging. Evaluation of the size distribution was performed by manually measuring single AuNPs from the TEM micrographs. The data were then transferred and analyzed using Microsoft Excel (2010).

The hydrodynamic diameter and agglomeration of the particles in suspension, i.e. diluted in distilled water (dH_2O), was evaluated with nanoparticle tracking analysis (NTA). The

calculation and analysis of three independent samples of each particle size was performed by our partners at LIST using a NanoSight ™ instrument (Version 2.3 Build 0033) (Malvern Instruments, Amesbury, UK).

2.2 Zebrafish maintenance and breeding

Zebrafish maintenance and exposure studies were performed at the Model Fish Unit (MFU) at the Section for Experimental Biomedicine, Department of Production Animal Clinical Sciences, Norwegian University of Life Sciences (NMBU) which has been accredited by the Association for Assessment and Accreditation of Laboratory Animal Care International (AAALAC) since 2008.

Adult zebrafish were kept in aquarium at 26-30 °C, with a 14:10 hour light: dark cycle. The aquarium water, hereafter system water, consisted of 60 mg/L Instant Ocean (Aquarium systems, Maryland, USA) in reverse osmosis water at a pH of 7.0 ± 1.0. The physical parameters of the system water, such as the pH, the general hardness and ammonium levels were recorded on a daily basis, and are important in maintaining a healthy stock of fish.

The in-house stocks of adult zebrafish from the AB wild type (wt) strain were bred to obtain a sufficient amount of embryos for the exposure studies. Breeding was performed by transferring two males and three females to 2 L breeding tanks. A transparent barrier was placed in the tank to separate males and females and a small handful of marbles was placed in the compartment containing the females to mimic natural spawning grounds. The tanks were left overnight and the barriers were removed the following morning. The fish were left to spawn for 0.5- 0.45 hours. After the spawning period, fertilized eggs from the breeding tanks were collected using a sieve and embryos were pooled together in a petri dish (<100 per dish). The collected embryos were immediately rinsed with autoclaved system water (embryo water), before they were transferred to new petri dishes. The embryos were reared in petri dishes until 120 hours post fertilization (hpf) and incubated at 28 °C. Dead individuals were removed and embryo water was changed on a daily basis.

2.3 Microinjection in zebrafish

Microinjections in zebrafish were performed using a micromanipulator (Narishige EG-400, Tokyo, Japan) which was connected to a Picospritzer III (Parker Hannfin Corp, Cleveland, OH, USA) nitrogen pressure system. Borosilicate needles for injection with a 1 mm outer diameter x 0.78 mm inner diameter (Harvard apparatus, Holliston, MA, USA), were prepared with a micropipette puller machine (Flaming/Brown, P-97, Sutter Inc. Novato, CA, USA) using program 3 for fine-tipped needles. The needle was loaded with 6 - 10 µl of the test suspension and then attached to the micromanipulator connected to the pressure system. The needles were unsealed by clipping the tip with sharp forceps and trial injections were made in mineral oil (Sigma-Aldrich, St. Louis, MO, USA). The diameter of the produced droplet was measured with a 1 mm ruler incorporated on a glass slide and the settings on the pressure system were adjusted to achieve an injection volume of approximately 1 nl for all exposures.

Trial injections in embryos and larvae were conducted prior to the experiments with 1% phenol red (Sigma-Aldrich) in phosphate buffered saline (Lonza, Basel, Switzerland) to verify that injections were performed correctly. Injections in larvae (48 – 72 hpf) were made into the duct of Cuvier for a systemic exposure, and were considered successful if the phenol red could be seen in the circulation following injection.

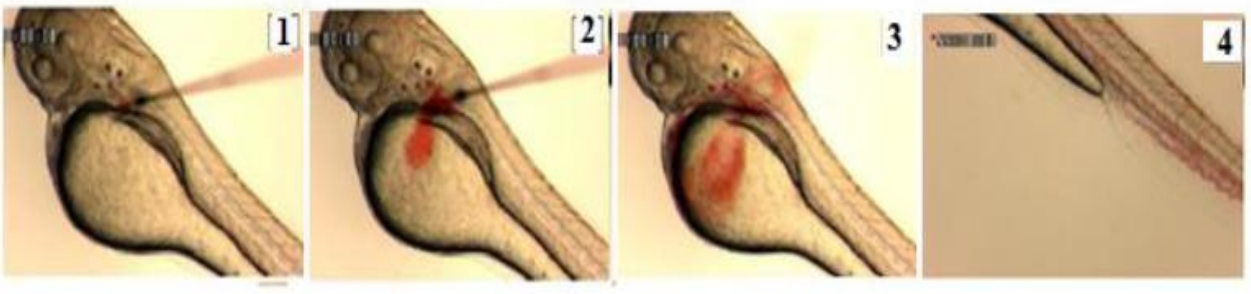

Figure 1. *Microinjection in zebrafish embryo. Phenol red is seen in the systemic circulation following injection into the duct of Cuvier. This figure was made by David Westmorland during his master thesis in Gareth Griffiths group (UiO).*

2.4 Survival assessment

Survival of zebrafish exposed to 20, 40 or 80 nm AuNPs was assessed at 100 hpf in zebrafish injected at the embryonic stage (2-4 hpf) or at the larval stage (72 hpf) [1].

The stock suspensions of the AuNPs were gently vortexed (IKA ® MS1Shaker, Sigma-Aldrich) for 10 seconds at low speed prior to dilution. Distilled water (dH_2O) was used to prepare the particle suspensions to yield experimental concentrations of 5, 50, 100, 500 and 1000 μg/ml of each particle size. In addition, two controls groups were included and consisted of embryos that were injected only with dH_2O for comparisons with the AuNP treated fish, and a non-injected/untreated control. The latter was included to assess the egg quality and to compare the potential effects of the microinjection procedure in the dH_2O-injected groups. Overall, a survival rate of >90% in the negative controls is required for valid tests in the fish acute toxicity test (TG 236, OECD).

At 2-4 hpf, zebrafish embryos were placed on 1% agarose plates (VWR, Letterworth, UK) and injected directly into the yolk sac with 1 nl of the test solutions. At 72 hpf larvae, from the same batch, were anesthetized (as described in section 2.6.2) and injected with 1 nl of the particle suspension into the duct of Cuvier. After injections, twenty individuals from each treatment group and the controls were transferred to individual wells on a 96-well plate. The embryos were distributed between two plates as illustrated in figure 2.2**.** The wells were filled with 250 μl of embryo water and were cleaned on a daily basis by replacing with 50 % of the embryo media (125 μl) with fresh solution. The plates were then placed in an incubator and kept at 28 °C.

At 100 hpf, several observations were recorded in larvae and embryo as indicators for mortality, including the coagulation of fertilized eggs, lack of heartbeat, no movement and

[1] Note that a distinction is made here between embryo and larvae to separate between the two developmental time points chosen for the survival studies. Generally, zebrafish up to 120 hpf are referred to as embryos. They are described as larvae in this context because they are hatched and swimming at 72 hpf.

unresponsive to touch stimuli. The experiment was repeated three times using different batches of fish.

	1	2	3	4	5	6	7	8	9	10	11	12
A	D	D	D	D	D	D	D	D	D	D	—	—
B	1000	1000	1000	1000	1000	1000	1000	1000	1000	1000	—	—
C	500	500	500	500	500	500	500	500	500	500	—	—
D	100	100	100	100	100	100	100	100	100	100	—	—
E	50	50	50	50	50	50	50	50	50	50	—	—
F	5	5	5	5	5	5	5	5	5	5	—	—
G	C	C	C	C	C	C	C	C	C	C	—	—
H	—	—	—	—	—	—	—	—	—	—	—	—

Figure 2. *Experimental setup for the survival study. Twenty injected embryos from each treatment group and the controls were distributed between two 96-well plates, for each particle size, with each well containing one zebrafish. Numbers represent the injected dose in μg/ml; D= distilled water control; C= untreated control; dashed line (—) = blank wells.*

2.5 Immune response

All procedures regarding the methods for assessing the immune response were performed following protocols that were developed at The Department of Pharmaceutical Biosciences at the University of Oslo. Microinjections and sampling was performed at MFU, NMBU, while the RNA extraction and gene expression analysis (qPCR) was conducted at UiO.

2.5.1 Microinjection of gold nanoparticles

Particle suspensions of 20, 40 and 80 nm AuNPs were prepared prior to exposure (as described in section 2.5), to yield experimental concentrations of 0.1, 0.5 and 1.0 μg/ml of each particle size. In addition, two control groups were included that consisted of embryos injected only with dH_2O and an untreated control group.

Because the innate immune system in zebrafish is not fully present until approximately 48 hpf (Herbomel et al., 1999) and it was decided to inject at 72 hpf for the immune response assessment. Microinjection in zebrafish a time consuming procedure and the injection of the different particle sizes were therefore performed at separate time points using different batches of fish. The choice of concentrations for the immune response was largely based on a pilot study that was performed in zebrafish embryo injected with 20 nm AuNPs (presented in Appendix B) and were considered as sub-lethal based on prior survival assessments.

Zebrafish embryos were anaesthetized at 72 hpf using approximately 3-4 ml buffered tricaine methanesulfonate solution (5 mg/mL) (MS 222, Finquel; Argent Laboratories Group, Inc. Redmond, WA, USA) in embryo water. The pH of the tricaine solution was adjusted to 7.5± 0.5 using Trizma® base (Sigma-Aldrich). After 1-2 minutes, anesthetized embryos were transferred to 1% agarose plates and any excess water was removed to immobilize the fish. Injection of the particle suspensions were made into the duct of Cuvier under a stereomicroscope (Wild M10, Leica microsystems GmbH, Wetzlar, Germany), and approximately 30 embryos were injected per treatment group. After injections, the embryos were transferred new petri dishes, containing fresh embryo water and were kept at 28° C until RNA isolation.

2.5.2 Sampling of material for gene expression analysis

Samples for gene expression analysis were collected at 2, 24 and 48 hours post injection (hpi). The selection of the time points was chosen to assess the immediate response, and the changes in gene expression following exposure. A limit for using zebrafish embryos in experiments is set at 120 hpf, which corresponds to 48 hpi in this study. At each time point, nine randomly chosen zebrafish embryos from each treatment group were euthanized by an overdose of tricaine solution. Three embryos were pooled into one sample, and the total number of replicates for each treatment group and the controls, at each time point, was three (Table 1). Embryos were transferred to 1.5 ml Eppendorf tubes

(Hamburg, Germany) and the embryo water was immediately removed and replaced by 200 µl RNAlater (Ambion ® by Life Technologies ™, Carlsbad, CA, USA), which was used to stabilize and preserve the RNA in the samples. The samples were kept for long-term storage at 4°C until the extraction of RNA.

Table 1. *Total amount of replicates in each treatment group for the immune response. Each replicate consisted of 3 embryos pooled together. The total number of zebrafish embryos used in the experiment was therefore 297(=11 treatments x 3 time points x 3 replicates x 3 individuals)*

Particle size	Treatment *	2 hpi	24 hpi	48 hpi
20 nm AuNPs	0.1 µg/ml	3	3	3
	0.5 µg/ml	3	3	3
	1.0 µg/ml	3	3	3
40 nm AuNPs	0.1 µg/ml	3	3	3
	0.5 µg/ml	3	3	3
	1.0 µg/ml	3	3	3
80nm AuNPs	0.1 µg/ml	3	3	3
	0.5 µg/ml	3	3	3
	1.0 µg/ml	3	3	3
Control	dH_2O-control	3	3	3
	Untreated	3	3	3

* The injection volume was 1 nl for all exposures

2.5.3 Extraction of total RNA

The RNAlater was removed and replaced by 600 µL buffer RLT (provided in RNeasy Mini Kit, QIAGEN, GmBH, Hilden, Germany), which was supplemented with 2-mercptoehtanol (10 µl/ml) (Invitrogen, Paisley, UK) to eliminate ribonuclease (RNase) released during homogenization. Disruption of the samples was performed using a mortar and pestle (Sigma-Aldrich) and the lysate was passed a minimum of five times through a 27 gauge x 1 needle fitted to a 5 ml syringe (BD, Franklin Lakes, NJ, USA). The samples were then centrifuged at 15 000 rpm for 3 minutes (Mikro200R, Hettich, Buckinghamshire, UK) and the RNA-containing supernatants was transferred into new 1.5 ml Eppendorf tubes and

mixed with 600 µL of 70% ethanol (Kemetyl, Vestby, Norway). The samples were loaded into RNEasy Mini Spin columns (QIAGEN) and centrifuged for another 15 seconds.

The isolation of the RNA was performed with the RNeasy Mini Kit (QIAGEN) following the manufacture's protocol (Appendix B: Kit protocols). The process involves a 15-minute deoxyribonucease (DNase) treatment, which was performed using an RNase-free DNase set (QIAGEN) to remove DNA from the samples. After the DNase treatment, 500 µl buffer RPE was added to each spin column and centrifuged in two subsequent steps to remove salts from the previous buffer treatments. Spin columns were then transferred to new collection tubes and centrifuged for another 2 minutes to remove traces of ethanol.

The spin columns were transferred to new collection tubes and, finally to elute the RNA, 20 µl Milli-Q water (Merck Millipore, Billerica, MA, USA), was added to each spin column membrane, giving a total RNA volume of 20 µl. The RNA quantity and quality in the samples were measured with a Picodrop spectrophotometer (PICOPET01, Picodrop Ltd., Cambridge, UK) and were analyzed using the Picodrop microlite software (release V2.07). The integrity of the isolated RNA was determined by the 260/280 and 260/230 nm spectrum ratios, with an acceptance value of ~2.0. The samples were stored at - 80°C until reverse transcription reactions.

2.5.4 Reverse transcription: cDNA synthesis

The reverse transcription (RT) reactions were performed with a High Capacity RNA-to-cDNA Kit (Applied Biosystems by Life Technologies ™) and a maximum of 9 µl RNA was used for each reaction. For each sample 10 µL RT buffer, 1 µl enzyme mix and 9 µl RNase-free water (provided in the kit) was added to give a total reaction volume of 20 µl. In addition, negative controls were included to confirm the absence of DNA contamination in the samples**.** The RT incubation reaction was performed using the GeneAmp PCR System (2700 PCR machine, Applied Biosystems) and consisted of 1 hour at 37 °C. The reaction was then stopped by heating to 95°C for 5 minutes and held at 4 °C. The cDNA was kept at -80°C until quantitative PCR (qPCR).

2.5.5 Primers and quantitative PCR

Validated zebrafish primers were obtained from commercial suppliers (table 2.7) and were chosen to represent a wide range of inflammatory responses in the zebrafish (Brudal et al., 2014). TNF-α, IL-1β, IL-8, IL-12a and INFg1-2 were chosen to represent proinflammatory cytokines and IL-10 was chosen as an anti-inflammatory cytokine. The reference genes 18S rRNA and EF1α were included to normalize the relative transcription levels and have been reported to be stable during zebrafish development (Tang et al., 2007).

Table 2. *Selected primers used for qPCR in for the immune response*

Gene name	Gene symbol	Function	Manufacturer *
18S rRNA	*zgc: 158463*	Reference gene	Invitrogen
Elongation factor 1-alpha	*ef1a*	Reference gene	Invitrogen
Tumor necrosis factor a	*tnfa*	Proinflammatory	QIAGEN
Interleukin 1, beta	*il1b*	Proinflammatory	QIAGEN
Interleukin 8	*il8*	Anti-inflammatory	QIAGEN
Interleukin 10	*il10*	Proinflammatory	QIAGEN
Interleukin 12a	*il12a*	Proinflammatory	QIAGEN
Interferon, gamma 1-2	*ifng1-2*	Proinflammatory	QIAGEN

* Forward and revers primers from Invitrogen are provided in separate tubes

The cDNA was diluted in RNase-free water in a 1:10 ratio. A SYBR ® Green (Roche, Basel, Switzerland) master mix was prepared for each primer pair (described in Appendix A). For each reaction 15 µl master mix and 5 µl diluted cDNA was added, to obtain a total volume of 20 µl. Quantitative PCR was performed in triplicates using a LightCycler ® 480 (Roche) qPCR machine. The LightCycler was set at the following conditions for the qPCR: 5 minutes denaturation at 95 °C, 45 cycles amplification with 10 seconds at 95 °C, 30 seconds at 60 °C and 8 seconds at 72 °C. The produced melting peaks and amplification curves were analyzed with the LightCycler ® 480 software to evaluate the primer specificity and the cycle threshold values, respectively. The absence of multiple peaks observed on the

individual melting curves indicates the primer-specific amplification of the PCR products (Figure 2.3 a).

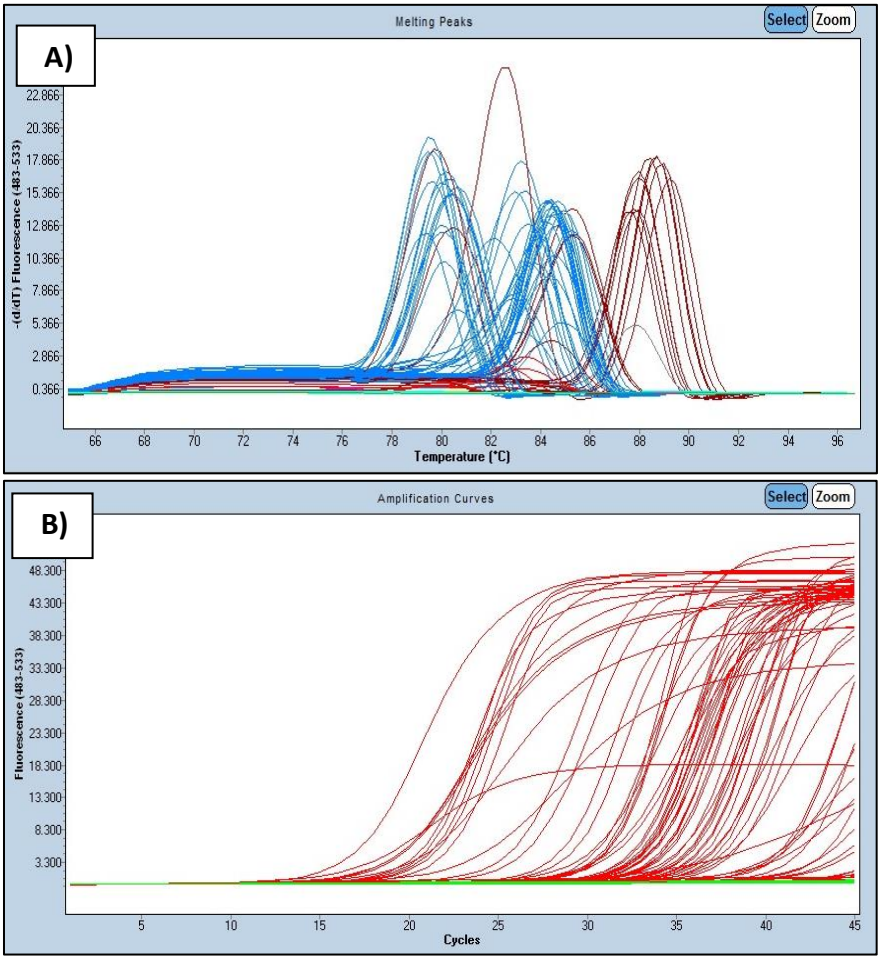

Figure 3. *Representative images from a qPCR run measuring the expression of inflammatory cytokines (A) Melting curves indicating primer-specific binding by the absences of multiple peaks in the individual samples, and (B) amplification curves reflecting the cycle threshold values*

The cycle threshold (C_t) values were analyzed in Microsoft Excel (2010) and represent the cycle number at which a signal is detected in the qPCR reaction. In general, a lower Ct value indicates a larger amount of cDNA in a sample, and is inversely related to the original expression level of the gene in interest (Bustin 2000).

The relative transcription level for each gene in each sample was determined by normalizing the C_t value against the primer efficiency (Brudal et al., 2013) using the following equation:

$$2^{\wedge} (C_{t\ max\ (primer)} - C_{t\ (sample)})$$

A normalization factor (N_F) was calculated by geometric averaging the mean of the two reference genes (Vandesompele et al., 2002) *18S* and *ef1a*. The relative transcription was then normalized against the N_F for each sample. The resulting normalized immune response data for the AuNP-treated fish was then standardized against the transcription levels in the dH_2O controls at each time point.

2.6 Statistical analysis

TEM measurements of the size distribution of the gold nanoparticles were evaluated with the statistical package R-3.2.0 (The R foundation, Vienna, Austria) using a general linear model (GLM) with particle size as the independent variable, and the TEM measurements as the dependent variables.

The statistical analysis of survival and immune data was performed using JMP 11 (SAS Institute Inc., Cary, NC, USA). The survival of zebrafish at 100 hpf was entered as a categorical variable (1= alive, 0= dead). Differences between the treatment groups and the control were analyzed using Fisher's exact test.

The distribution of the immune response data was investigated using Shapiro-Wilks test for normality, which revealed a skewed distribution for all the inflammatory genes. The log-transformed response, i.e. the transcription of inflammatory genes, gave a satisfactory fit to the normal distribution and was therefore used for the statistical analysis of the immune response data. General linear models were used, and the log-transformed

transcription data of inflammatory genes were dependent variables. Independent, categorical variables were exposure concentrations, particle sizes, time points after exposure and the interaction between particle size and time points was included in the model. Due to the small size of the dataset, it was decided to not investigate other potential interactions. The differences between treatment groups and the controls were evaluated using the *post hoc* Tukey's HSD for multiple comparisons.

Data are presented as the mean ± the standard error of the mean (SEM) and P values <0.05 are considered as statistically significant, unless stated otherwise.

3. Results

3.1 Characterization of gold nanoparticles

The transmission electron microscopy (TEM) images of 20 nm, 40 nm and 80 nm AuNPs showed that the particles were mostly round in shape, with some irregular morphology (triangular and oval) seen in all samples. The particles size measured by TEM were 20.5±0.4, 39.7±0.6 and 82.5 ±1.2 nm (mean ± SEM, *n*= 50) for the 20, 40 and 80 nm AuNPs, respectively, and were verified to be from significantly different size distributions ($p<0.001$ using GLM). The histograms produced from 50 random measurements showed a slightly skewed distribution for all particle sizes (Fig. 5-7).

The mean hydrodynamic diameter of the AuNPs in distilled water was measured by nanoparticle tracking analysis (NTA) and was reported to be 31±2.6, 50±3.2, 83±5.5 nm (mean ± SEM) for the 20, 40 and 80 AuNPs, respectively. The absence of multiple peaks is suggestive of little to no agglomeration in nanoparticle samples (Fig. 4).

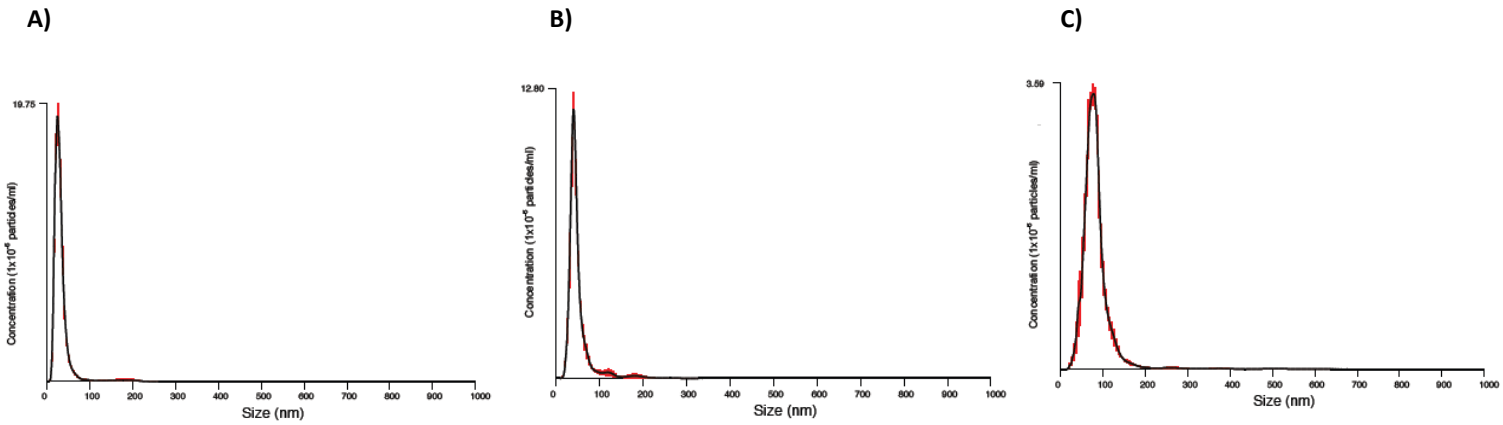

Figure 4. *Size distribution of AuNPs from NTA measurements: (a) 20 nm (b) 40 and (c) 80 nm AuNPs. Results are shown as the mean size distribution of three samples and the red line indicates the standard error of the mean (SEM). The y-axis is the volume distribution of the AuNPs in 1x 10 $^{-6}$ per ml distilled water.*

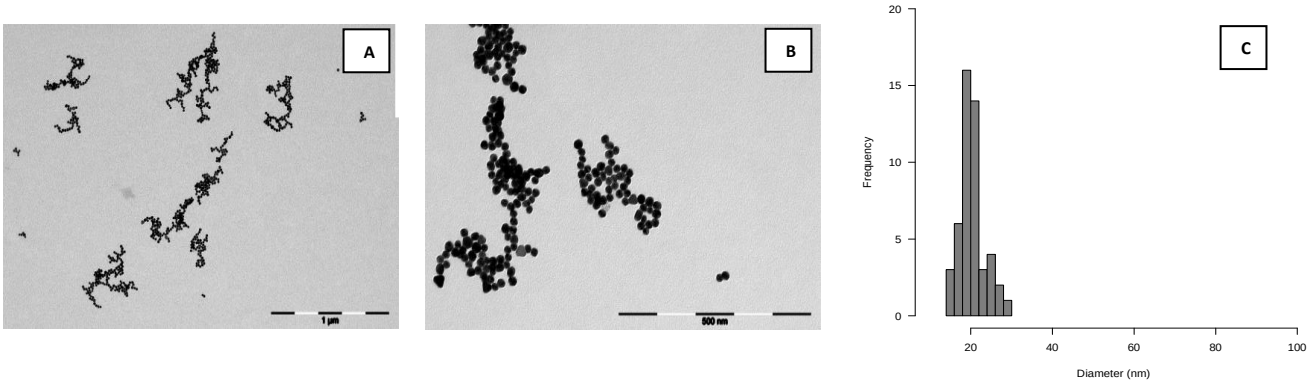

Figure 5. *TEM images and histogram of 20 nm AuNPs (a) representative image of the dispersity in the sample, the scale bar is 1 μm (b) an image at a higher magnification showing particle morphology, the scale bar is 0.5 μm (c) and histogram of the calculated size distribution (n=50).*

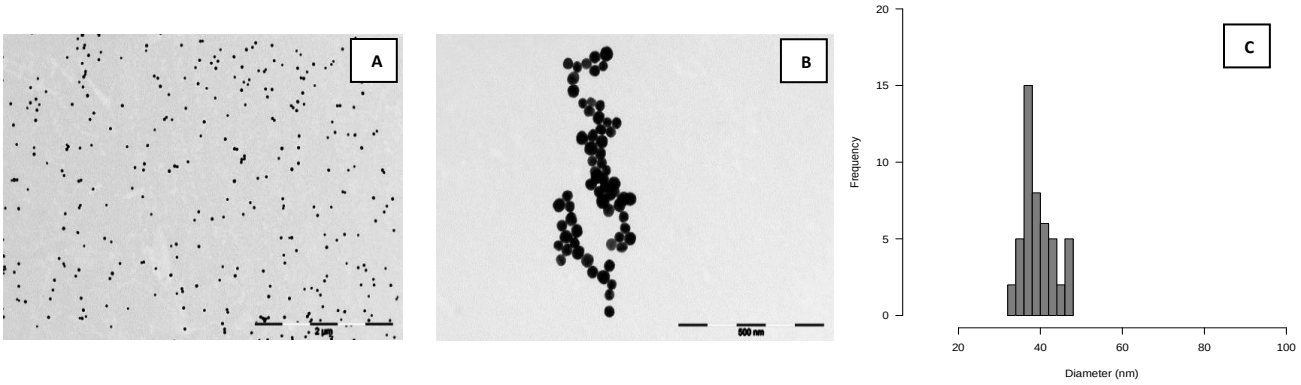

Figure 6. *TEM images and histogram of 40 nm AuNPs (a) representative image of the dispersity of the sample, the scale bar is 2 μm (b) an image at a higher magnification showing particle morphology, the scale bar is 0.5 μm (c) and histogram of the calculated size distribution (n=50).*

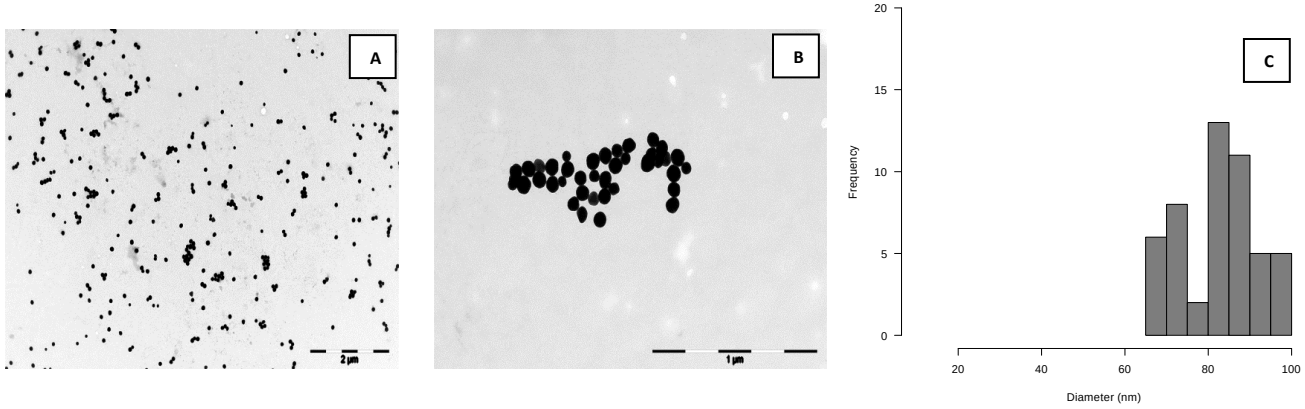

Figure 7. *TEM images and histogram of 80 nm AuNPs (a) representative image of the dispersity of the sample, scale bar is 2 μm (b) an image at a higher magnification showing particle morphology, the scale bar is 1 μm (c) and histogram of the calculated size distribution (n=50).*

3.2 Survival assessment

The survival of zebrafish embryos and larvae injected with 20, 40 or 80 nm AuNPs was assessed at 100 hours post fertilization. A significant decrease in survival was found in embryos exposed to 100, 500 and 1000 µg/ml of 80 nm AuNPs (Figure 7.c). In larvae, a significant, positive effect on survival was observed in zebrafish treated with 50 and 100 µg/ml 20 nm AuNPs (Figure 6.a). Although not statistically significant, a similar positive trend was observed in larvae exposed to 80 nm AuNPs. No significant difference in survival was observed between the untreated and dH_2O-injected control fish, suggesting that the process of injection does not affect survival at 100 hours post fertilization.

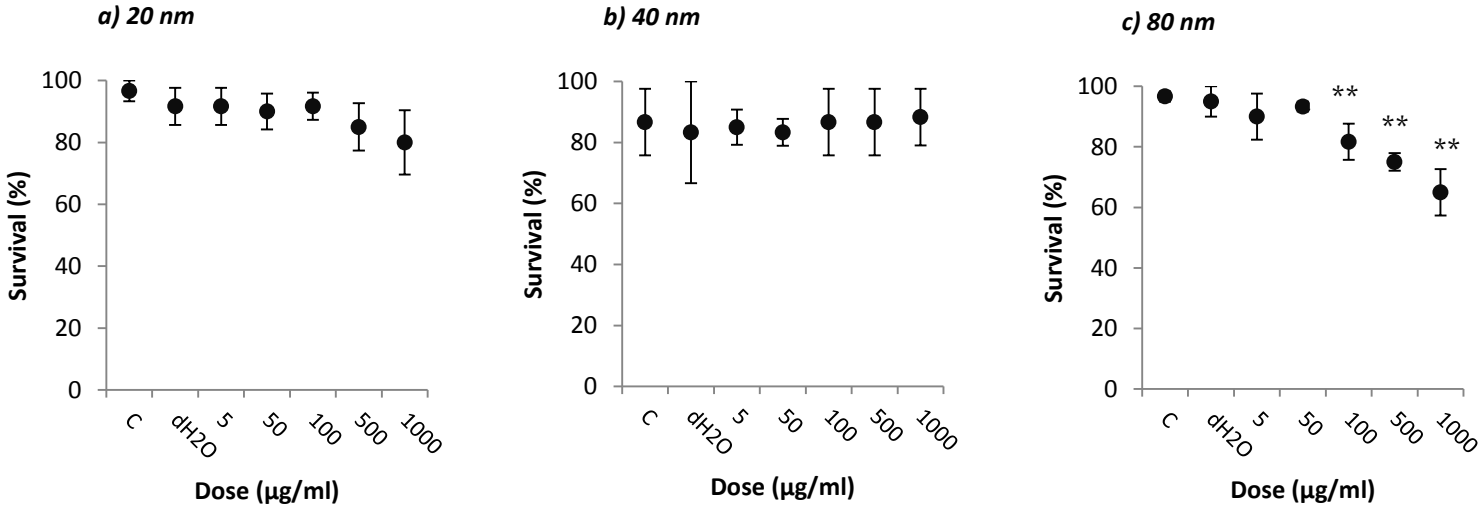

Figure 8. *Survival at 100 hpf of embryo injected at 2 -4 hpf with: (a) 20 nm AuNP (b) 40 nm AuNP and (c) 80 nm AuNP. Abbreviations: C=untreated; dH_2O= water injected control. Data are presented as the mean ± SEM (n=3). ** Significantly different from dH_2O control ($p<0.05$ using Fisher's exact test)*

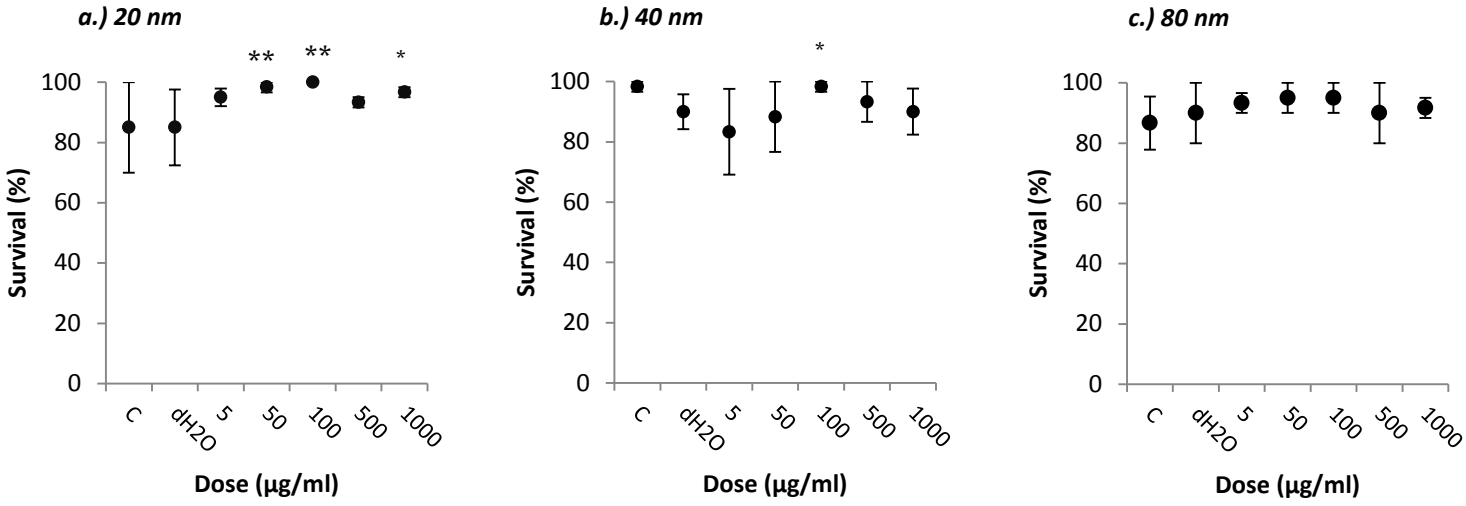

Figure 9. *Survival at 100 hpf of larvae injected at 72 hpf with: (a) 20 nm AuNP (b) 40 nm AuNP and (c) 80 nm AuNPs. Abbreviations: C=untreated; dH_2O= water injected control. Data are presented as the mean ± SEM (n=3). Symbols indicate a significant difference from dH_2O control (**p<0.05 and *p<0.1 using Fisher's exact test)*

3.3 Expression of inflammatory genes

Changes in expression of the selected inflammatory genes in zebrafish injected with gold nanoparticles were measured at 2, 24 and 48 hours post injection (hpi) by RT-qPCR. The relative transcription levels for the investigated genes TNF-α, IL-1β, IL-8, IL-10, IL-12a and IFNγ are presented in Fig. 10, and the parameter estimates with *p*-values from the GLMs of the log-transformed responses are presented separately in table 3-8. Overall, the results suggest that the gold nanoparticles tested induced changes in the expression of the examined inflammatory genes. The expression appeared to be transient, as the mean transcription level of all the proinflammatory genes was observed to be close to control levels by 48 hpi.

Time points

The results showed a significant increase in transcription of all the inflammatory genes at 2 hours post injection (Fig. 10) compared to the controls (table 3-8). The highest mean transcription levels observed were for TNF-α and IFNγ, while the lowest were observed for IL-10 in groups exposed to 80 nm AuNPs. The expression of TNF-α, IL-1β, IL-12a and IFNγ exhibited a similar time-course pattern, with expression at 2 hpi being significantly higher than at 24 and 48 hpi. However, IL-10 was significantly lower at 24 hpi, compared to 48 hpi. In addition, IL-8 showed high levels of expression at 24 hpi, being greater than, or equal to the levels at 2 hpi for 20 nm and 80 nm, respectively.

Particle size

An overall significant effect of particle size was observed for TNF- α, IL-1β and IL-10, with 80 nm AuNPs inducing a higher response compared to 20 nm AuNPs. For IFNγ, similar expression levels were observed for 40 and 80 nm AuNPs, with lowest levels observed for 20 nm.

Exposure concentration

A significant effect of the dose was observed for all the inflammatory genes (table 3-8), with the exception of TNF-α. There was a tendency for the highest dose to elicit the highest response. However, this was not consistent at every time point and the results showed no significant dose-dependent patterns, although opposite trends were observed at 2 hpi for IL-10 and IFNγ in zebrafish exposed to 80 nm AuNPs.

Interaction

Transcription at the various time points after exposure was different depending on the particle size. The transcription of TNF-α, IL-1β and IFNγ was considerably lower in groups treated with 20 nm AuNPs at 2 hpi compared to large sized particles. The interaction between particle and time was found to be a significant for the expression of TNF-α, IL-1β, IL-8 and IFNγ. As is apparent from the adjusted R^2 values (Table 3-8), the chosen model accounts for only approximately 50 % of the observed variation, which can be explained by exclusion of other interactions in the statistical model.

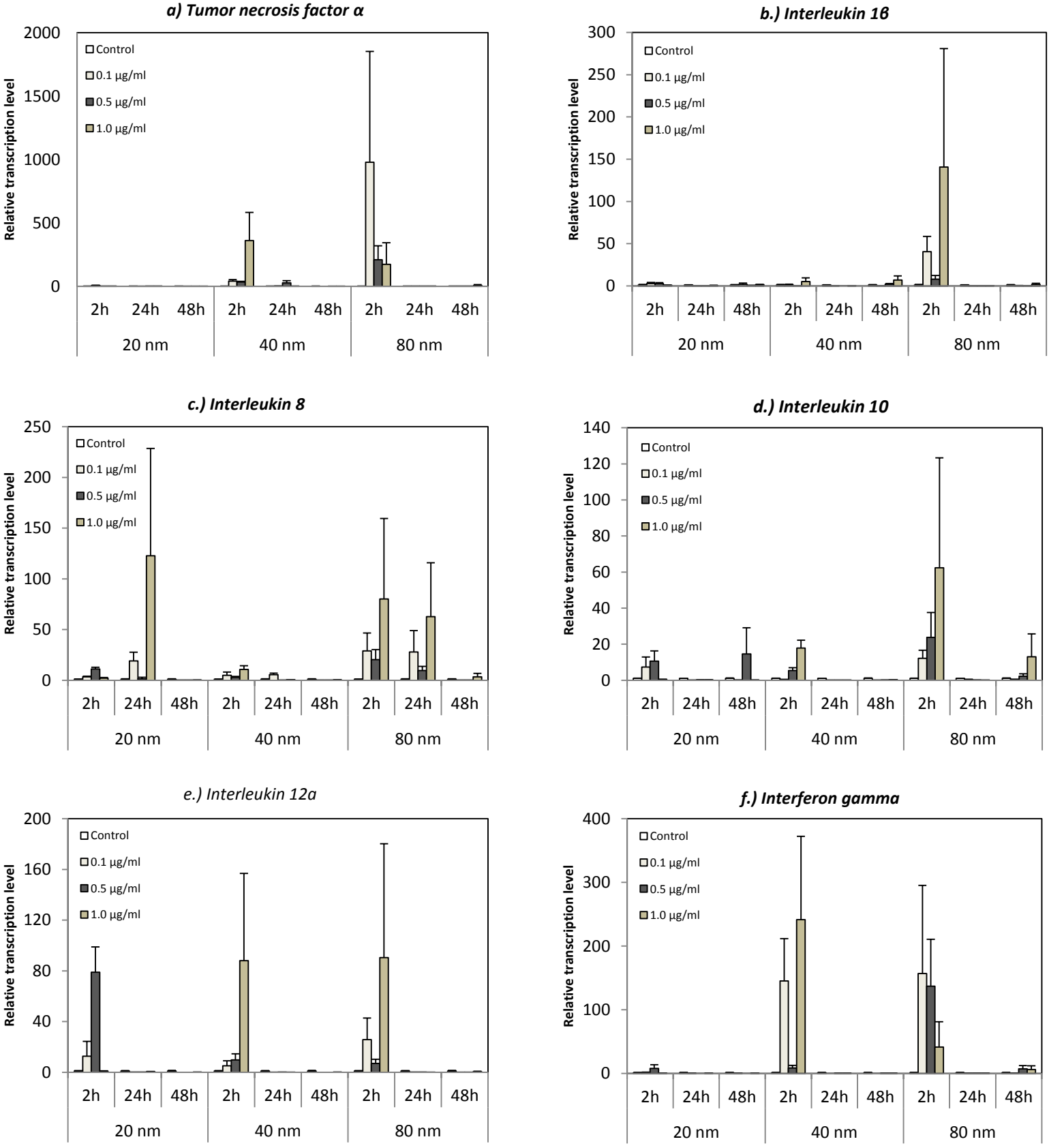

Figure 10. *Relative expression levels at 2h, 24h and 48h= hours post injection of the selected inflammatory genes (a) tumor necrosis factor α (b) interleukin 1β (c) interleukin 8 (d) interleukin 10 (e) interleukin 12a and (f) interferon gamma. Zebrafish were injected into the duct of Cuvier at 72 hpf with 0.1, 0.5 or 1.0 µg/ml of 20, 40 or 80 nm AuNPs. The relative expression was normalized against the two reference genes 18S rRNA and elongation factor 1-alpha, and were standardized against the transcription level of the dH_2O- injected controls at each time point. Data are presented as mean ± SEM (n=3).*

Table 3. *Parameter estimates for TNF-α with standard errors (SE), sums of squares (SS) and degrees of freedom (df) from the one-way ANOVA for the impact of particle size, dose, time and the interaction between particle and time on the log-transformed relative expression of TNF- α in zebrafish injected with AuNPs at 72 hpf. Ref. indicates the reference level used within each independent variable, and is arbitrarily selected by the statistical program.*

Response	Model		Adjusted R^2	df	Parameter estimates	SE	SS	*p*-value
Relative transcription LOG TNF-α		Intercept	0.532		-0.243	0.09		0.0082*
	Particle size	20 nm		2	-0.443	0.127	13.06	0.0008*
		40 nm			0.037			0.769
		80 nm			Ref.	Ref.		Ref.
	Dose	0		3	0.067	0.155	2.63	0.665
		0.1 µg/ml			-0.031			0.84
		0.5 µg/ml			Ref.	Ref.		Ref.
		1.0 µg/ml			-0.231			0.14
	Time	2 hpi		2	1.155	0.127	81.56	<0.0001*
		24 hpi			-0.215			0.093
		48 hpi			Ref.	Ref		Ref.
	Particle x Time	20 nm x 2hpi		4	-0.344	0.18	19.05	0.058
		20 nm x 24hpi			0.140			0.435
		40 nm x 2hpi			0.366			0.0445*
		40 nm x 24hpi			0.380			0.0370*

Table 4. *Parameter estimates for IL-1β with standard errors (SE), Sums of squares (SS) and degrees of freedom (df) from the one-way ANOVA for the impact of particle size, dose, time and the interaction between particle and time on the log-transformed relative expression of IL-1β in zebrafish injected with AuNPs at 72 hpf. Ref. indicates the reference level used within each independent variable, and is arbitrarily selected by the statistical program.*

Response	Model		Adjusted R^2	df	Parameter estimates	SE	SS	*p*-value
Relative transcription Log IL-1β		Intercept	0.433		-0.424	0.071		<.0001*
	Particle size	20 nm		2	0.179	0.101	2.64	0.079
		40 nm			-0.201			0.0489*
		80 nm			Ref.	Ref.		Ref.
	Dose	0		3	0.294	0.123	7.08	0.0194*
		0.1 µg/ml			-0.164			0.187
		0.5 µg/ml			Ref.	Ref.		Ref.
		1.0 µg/ml			0.199			0.11
	Time	2 hpi		2	0.587	0.101	35.9	<.0001*
		24 hpi			-0.783			<.0001*
		48 hpi			Ref.	Ref.		Ref.
	Particle x Time	20 nm x 2hpi		4	-0.269	0.143	9.23	0.063
		20 nm x 24hpi			0.362			0.1680*
		40 nm x 2hpi			-0.198			0.168
		40 nm x 24hpi			-0.185			0.198

Table 5. *Parameter estimates for IL-8* ***with*** *standard errors (SE), sums of squares (SS) and degrees of freedom (df) from the one-way ANOVA assessing the effect of particle size, dose, time and the interaction between particle and time on the log-transformed relative expression of IL-1β in zebrafish injected with AuNPs at 72 hpf. Ref. indicates the reference level used within each independent variable, and is arbitrarily selected by the statistical program.*

Response	Model		Adjusted R^2	df	Parameter estimates	SE	SS	*p*-value
Relative transcription Log IL-8		Intercept	0.43		0.01	0.073		0.8914
	Particle size	20 nm		2	-0.007	0.104	2.96	0.9442
		40 nm			-0.199			0.0589
		80 nm			Ref.	Ref.		Ref.
	Dose	0		3	-0.135	0.127	5.8	0.2907
		0.1 µg/ml			0.205			0.1102
		0.5 µg/ml			Ref.	Ref.		Ref.
		1.0 µg/ml			0.24			0.0629
	Time	2 hpi		2	0.53	0.104	39.31	<.0001*
		24 hpi			0.318			0.0034*
		48 hpi			Ref.	Ref.		Ref.
	Particle x Time	20 nm x 2hpi		4	-0.096	0.147	6.42	0.514
		20 nm x 24hpi			0.236			0.1124
		40 nm x 2hpi			0.122			0.4067
		40 nm x 24hpi			-0.468			0.0020*

Table 6. *Parameter estimates for IL-10 with standard errors (SE), Sums of squares (SS) and degrees of freedom (df) from the one-way ANOVA for the impact of particle size, dose, time and the interaction between particle and time on the log-transformed relative expression of IL-10 in zebrafish injected with AuNPs at 72 hpf. Ref. indicates the reference level used within each independent variable, and is arbitrarily selected by the statistical program.*

Response	Model		Adjusted R^2	df	Parameter estimates	SE	SS	*p*-value
Relative transcription LOG IL-10		Intercept	0.44		-0.322	0.066		<.0001*
	Particle size	20 nm		2	-0.07	0.094	4.26	0.4607
		40 nm			-0.20			0.0370*
		80 nm			Ref.	Ref.		Ref.
	Dose	0		3	0.292	0.116	6.45	0.0134*
		0.1 µg/ml			-0.371			0.0019*
		0.5 µg/ml			Ref.	Ref.	33.25	Ref.
		1.0 µg/ml			-0.039			0.7365
	Time	2 hpi		2	0.759	0.094		<.0001*
		24 hpi			-0.551			<.0001*
		48 hpi			Ref.	Ref.	2.16	Ref.
	Particle x Time	20 nm x 2hpi		4	-0.123	0.133		0.3593
		20 nm x 24hpi			0.217			0.1084
		40 nm x 2hpi			0.124			0.3557
		40 nm x 24hpi			-0.015			0.9106

Table 7. *Parameter estimates for IL-12a with standard errors (SE), Sums of squares (SS) and degrees of freedom (df) from the one-way ANOVA for the impact of particle size, dose, time and the interaction between particle and time on the log-transformed relative expression of IL-12a in zebrafish injected with AuNPs at 72 hpf. Ref. indicates the reference level used within each independent variable, and is arbitrarily selected by the statistical program.*

Response	Model		Adjusted R^2	df	Parameter estimates	SE	SS	*p*-value
Relative transcription LOG IL-12a		Intercept	0.58		-0.784	0.084		<.0001*
	Particle size	20 nm		2	0.0251	0.119	0.84	0.8331
		40 nm			-0.118			0.32
		80 nm			Ref.	Ref.		Ref.
	Dose	0		3	0.699	0.145	18.53	<.0001*
		0.1 µg/ml			-0.384			0.0099*
		0.5 µg/ml			Ref.	Ref.		Ref.
		1.0 µg/ml			-0.159			0.2771
	Time	2 hpi		2	1.375	0.119	104.33	<.0001*
		24 hpi			-0.515			<.0001*
		48 hpi			Ref.	Ref.		Ref.
	Particle x Time	20 nm x 2hpi		4	-0.096	0.168	2.38	0.5702
		20 nm x 24hpi			0.258			0.1289
		40 nm x 2hpi			0.158			0.3479
		40 nm x 24hpi			-0.138			0.4132

Table 8*. Parameter estimates for IFNγ with standard errors (SE), Sums of squares (SS) and degrees of freedom (df) from the one-way ANOVA for the impact of particle size, dose, time and the interaction between particle and time on the log-transformed relative expression of IFNγ in zebrafish injected with AuNPs at 72 hpf. Ref. indicates the reference level used within each independent variable, and is arbitrarily selected by the statistical program.*

Response	Model		Adjusted R^2	df	Parameter estimates	SE	SS	p-value
Relative transcription LOG IFNγ		Intercept	0.58		-0.862	0.106		<.0001*
	Particle size	20 nm		2	-0.419	0.15	15.23	0.0063*
		40 nm			-0.071			0.6333
		80 nm			Ref.	Ref.		Ref.
	Dose	0		3	0.67	0.184	5.3	0.0004*
		0.1 µg/ml			-0.491			0.0089*
		0.5 µg/ml			Ref.	Ref.		Ref.
		1.0 µg/ml			-0.011			0.95
	Time	2 hpi		2	1.595	0.15	59.24	<.0001*
		24 hpi			-1.113			<.0001*
		48 hpi			Ref.	Ref.		Ref.
	Particle x Time	20 nm x 2hpi		4	-0.291	0.212	16.68	0.174
		20 nm x 24hpi			0.365			0.0887
		40 nm x 2hpi			0.590			0.0066*
		40 nm x 24hpi			-0.065			0.7584

4. Discussion

The main objective was to determine whether exposure to AuNPs would elicit an inflammatory response in zebrafish, and to what extent the particle size would influence any response. The results provided support for our hypothesis, since an inflammatory response was indeed induced by AuNPs. In addition, moderate differences related to size were observed, with 80 nm AuNPs inducing the highest response with regards to survival and gene expression.

4.1 Characterization

The citrate stabilized gold nanoparticles (AuNPs) used in this thesis were confirmed to be mostly round in shape by TEM and the measured size distributions were within 10 % of the particle sizes declared by the supplier (Fig. 5 -6). The average sizes of the AuNPs measured by NTA were larger (Fig. 4), which is expected as the method measures the hydrodynamic diameter (Browning et al., 2012). However, the 20 and the 40 nm AuNPs were approximately 10 nm larger than the target size, which might suggest lower colloidal stability of the smaller particles. The NTA results revealed little to no aggregation of AuNPs in distilled water, which was indicated by the absence of multiple peaks. Both methods used for characterization resulted in size distributions different from the target values and highlights the importance of characterization. Size is suggested to play a key role in nanotoxicity (Oberdorster et al., 2005a), and as agglomeration may shift the size distribution towards larger sizes, it could lead to the misinterpretation of the results.

4.2 Zebrafish embryo survival

It has been shown in several studies that zebrafish are susceptible to toxic effects induced by nanoparticles (Lee et al., 2007). Our results demonstrated a modest effect on survival, with no AuNP-treatment associated with more than 35 % mortality at 100 hpf (Figure 3.2 – 3.3). This can be considered as moderate, as 10 % mortality is considered normal according to the ZFET test (OECD, TG 236) and can be attributed to random effects. Our results are in agreement with studies showing gold nanoparticles to be relatively nontoxic (Kovriznych et al., 2013), with several reports of low mortality in zebrafish embryos at the highest concentrations tested (Bar-Ilan et al., 2009; Asharani et al., 2011). Survival was only found to be significantly reduced in embryos exposed at 2-4 hpf to the highest doses of 80 nm AuNPs, which was the largest particle size tested. This is in contrast to *in vitro* findings that suggest higher toxicity of smaller sized AuNPs (Pan et al., 2009), which is often suggested for nanoparticles due to an increased surface reactivity with decreasing size (Oberdorster et al., 2005a; Tedesco et al., 2010; Yeo et al., 2010). Nevertheless, extrapolation from *in vitro* studies should be done with caution and it is likely that different sized particles exert toxicity through different mechanisms of action (Sohaebuddin et al., 2010). However, it was recently demonstrated in zebrafish that 82.2 nm AuNPs induce less embryonic lethality and developmental abnormalities compared to 11.6 nm AuNPs, when exposed through water (Browning et al., 2013). Our conflicting results with regards to larger sized AuNPs may reflect differences in the exposure route. Although not substantiated for in this study, our results might indicate higher toxicity of larger AuNPs when particles are delivered directly into the systemic circulation.

No significant, negative effect on the survival of larvae was found in this study. Embryonic stages have been shown to be more sensitive towards the toxic effects of nanoparticles compared to later stages (Brun et al., 2014) and AuNPs have been shown induce higher mortality in embryos, when compared to larvae in Japanese medaka (*Oryzias latipes*)(Shin et al., 2014). Our findings seem to be in support of these results, as survival was lower in embryos exposed to 80 nm AuNPs, compared to larvae exposed to the same doses. In addition, we observed opposite trends in embryos and larvae, with results suggesting a

positive effect on survival in larvae. However, these results can be explained by the higher mortality rates observed in the 20 nm larval control group, with 12 dead larvae recorded in one of the replicates. It should be noted that survival was only recorded at 100 hpf and not throughout the duration of the experiment. The results from AuNP treated embryos are however interesting, and appear to suggest differences in survival related to particle size.

4.3 Expression of inflammatory genes

Our results demonstrate that AuNPs significantly increased the transcription of all the inflammatory cytokines measured; TNF-α, IL-1β, IL-8, IL-10, IL-12a and IFNγ, in zebrafish at 2 hours post injection (hpi). The expression appeared to be transient, as the transcriptional levels were greatly reduced by 24 hpi and were close to control levels by 48 hpi for all genes, with the exception of IL-10. A slight increase in the transcription of IL-10 was observed at 48 hpi, but only in groups injected with 20 and 80 nm AuNPs. IL-10 is also known as cytokine synthesis inhibitory factor (CSIF) and is an anti-inflammatory cytokine which functions to suppress the transcription of proinflammatory cytokines (Zhang et al., 2005; Seppola et al., 2008). Although the differences were minor, the increased transcription of IL-10 at 48 hpi is interesting as it was the only anti-inflammatory gene included in this assessment and may suggest an immunomodulatory response.

The highest mean expression at 2 hpi was found for TNF-α and IL-1β in 80 nm AuNP treated groups and IFNγ for 40 and 80 nm AuNPs. Both TNF-α and IL-1β are considered as important indicators of phagocytic activity and they are the first cytokines produced in the initial stages of an inflammation, both in fish and in mammals (Roca et al., 2008). IFNγ has important antiviral and macrophage activating properties (Altmann et al., 2003), IL-8 is important in the recruitment of neutrophils (de Oliveira et al., 2013) and IL-12a functions in regulating the production of cytokines (Ito et al., 2008). These are the main proinflammatory cytokines produced by activated immune cells in zebrafish (van der Vaart et al., 2012) and the expression of the genes observed in our results, may therefore be interpreted as the stimulation of an immune response.

The time-dependent pattern in cytokine expression observed in this study is consistent with findings reported from studies with rodents. TNF-α and IL-1β have been shown to be transiently increased in rats injected intraperitoneally with 10 and 50 nm AuNPs (Kahn et al., 2013), with 50 nm inducing a more severe inflammation in the liver. In the present study, the expression of TNF-α, IL-1β and IFNγ was found to be considerably higher in groups exposed to 80 nm AuNPs compared to 20 nm and might indicate differences in expression that are related to particle size. The increase of TNF-α, IL-1β, IL-10 and IL-12 has been associated with acute liver inflammation and apoptosis in rats intravenously injected with 13 nm PEG-coated AuNPs (Cho et al., 2009). However, PEG surface coatings generally delay immune system recognition of NPs (Walkey et al., 2012) and comparison with such studies should be done with caution.

Microarray studies have shown that AuNPs functionalized to carry a charge significantly disturbs pathways involved in inflammation and the immune system in zebrafish (Truong et al., 2013) and zinc oxide NPs have been shown to induce the transcription of TNF-α, IL-1β and genes related to oxidative stress in zebrafish (Brun et al., 2014). The AuNPs used in in the present study were not functionalized, however, citrate stabilized AuNPs carry a slightly negative charge, which is unavoidable due to the methods used to synthesize gold colloids (Geffroy et al., 2012).The charge of gold nanoparticles is suggested to play an important role in AuNP toxicity (Truong et al., 2012; Kim et al., 2013), even more so than the dose, which has been reported to induce insignificant and stochastic developmental abnormalities in zebrafish embryo (Browning et al., 2009; Browning et al., 2013). Our results revealed no significant dose-dependent effects on transcription. There was a tendency for the highest dose to elicit the highest response and a dose-related trend was observed for IL-10 and IFNγ, however, these patterns were not consistent at every time point and particle size. The injected doses are low, compared with concentrations

The changes in gene expression reported in this study suggest a low inflammatory potential of the examined AuNPs, as a transient increase of inflammatory cytokines can be considered as a general response to injury in the host defense mechanism (de Oliveira et

al., 2013). The recruitment of neutrophils and macrophages are commonly associated with tissue injury in zebrafish (Herbomel et al., 1999; Sieger et al., 2009), which could explain the increase in cytokine production observed at 2 hpi. However, the transcription of cytokines was consistently lower in the control fish injected with dH_2O, which suggests that the time-dependent pattern observed in the AuNP treated fish is separate from the wound inflicted during microinjection.

4.3.1 Methodical considerations

Reverse transcription quantitative PCR (qPCR) was used to quantify changes in the gene expression in zebrafish following AuNP exposure, and is regarded as a sensitive method for measuring cytokines, which normally are expressed at low levels (Giulietti et al., 2001). There are several important factors to consider when using qPCR in effects assessment, including the use of reference genes as internal controls to normalize the transcription levels (Vandesompele et al., 2002). Optimally, reference genes should be stably expressed in all tissues and be unaffected by the experimental treatment (Bustin 2002). The selected reference genes in the present study, 18S rRNA and EF1a have previously been reported to be stably expressed during zebrafish development (Tang et al., 2007; McCurley et al., 2008; Brudal et al., 2013) and appeared to be unaffected by the AuNP treatment (data shown in appendix B.2). An increased expression of EF1a was observed at 48 hpi, however this pattern was consistent across all treatments, indicating that this was not an effect of AuNP exposure.

It should be noted that a considerable amount of variation was observed in the data, making the results difficult to interpret. A problem arises when there are only three biological replicates, and cytokine expression in individual zebrafish has been shown to be highly variable following bacterial infection (Rojo et al., 2007). Microinjection in 72 hpf zebrafish is a time consuming procedure and the amount of biological replicates that can be included using this method is therefore limited. For future reference it would be justified, and recommended to reduce the number of treatments for the purpose of increasing the sample size.

RT qPCR has been used successfully to evaluate the immediate and the chronic immune response following bacterial infection in zebrafish (Rojo et al., 2007; Brudal et al., 2014) and is becoming an established method for evaluating the inflammatory potential of nanoparticles, also in zebrafish (Jovanović et al., 2011; Brun et al., 2014). In the present study we demonstrated that the zebrafish model could be utilized for evaluating changes in the gene expression of inflammatory cytokines following a systemic exposure to AuNPs.

5. Conclusion

The present study demonstrated a transient increase of the inflammatory cytokines TNF-α, IL-1β, IL-8, IL-10, IL12a and IFNγ in zebrafish, primarily at 2 hpi following the systemic exposure to 20, 40 and 80 nm citrate stabilized AuNPs, indicating the stimulation of an immune response. Differences in gene expression were observed, with 80 nm AuNPs inducing higher levels of transcription of the proinflammatory genes TNF-a, IL-1β and IFNγ. This provides support to the initial hypothesis that AuNPs induce and immune response and that the immune response may be influenced by particle size.

The observed changes in transcription suggest a low inflammatory potential of gold nanoparticles, as a transient increase in cytokines may be regarded as a rather general immune response. For the biomedical purposes of AuNPs, a low inflammatory potential is desired. However, the observed differences related to particle size calls for further investigations, and studies on a higher biological level are required to fully evaluate the potential toxicity.

Future perspectives

In this study we examined the inflammatory effects of AuNP exposure on the molecular level in zebrafish, i.e. at the level of transcription. Studies on the molecular level are important to gain insight about the mechanisms of toxicity, but should be coupled with assessments on a higher biological level. Future investigations should utilize the potential of the various transgenic zebrafish lines that are available for the real-time observation of biological responses. Localization and cellular interactions with AuNPs and immune cells could be evaluated using transgenic lines that express fluorescence in macrophages and neutrophils. It was recently demonstrated in our research group that the AuNPs examined in the present study, induce behavioral changes in zebrafish. It would therefore be of particular interest to examine NP interactions with microglia cells, which are the resident macrophages in the central nervous system, to evaluate whether immune system pathways are involved in the observed behavioral effects. Further, to examine effects on survival, the immunological impact of developmental exposure to NPs could be assessed by the administration of a bacterial challenge, either during development or during a later stage in life.

References

Aillon, K. L., Xie, Y., El-Gendy, N., Berkland, C. J. and Forrest, M. L. (2009). "Effects of nanomaterial physicochemical properties on in vivo toxicity." *Advanced Drug Delivery Reviews* **61**(6): 457-466.

Alexis, F., Pridgen, E., Molnar, L. K. and Farokhzad, O. C. (2008). "Factors affecting the clearance and biodistribution of polymeric nanoparticles." *Molecular Pharmaceutics* **5**(4): 505-515.

Alkilany, A. and Murphy, C. (2010). "Toxicity and cellular uptake of gold nanoparticles: what we have learned so far?" *Journal of Nanoparticle Research* **12**(7): 2313-2333.

Altmann, S. M., Mellon, M. T., Distel, D. L. and Kim, C. H. (2003). "Molecular and functional analysis of an interferon gene from the zebrafish, Danio rerio." *Journal of Virology* **77**(3): 1992-2002.

AshaRani, P. V., Mun, G. L. K., Hande, M. P. and Valiyaveettil, S. (2009). "Cytotoxicity and Genotoxicity of Silver Nanoparticles in Human Cells." *ACS Nano* **3**(2): 279-290.

Asharani, P. V., Yi, L. W., Gong, Z. Y. and Valiyaveettil, S. (2011). "Comparison of the toxicity of silver, gold and platinum nanoparticles in developing zebrafish embryos." *Nanotoxicology* **5**(1): 43-54.

Balkwill, F., Mantovani, A. (2001). "Inflammation and cancer:back to Virchow?" *Lanclet* **357**(9255): 539-545.

Bar-Ilan, O., Albrecht, R. M., Fako, V. E. and Furgeson, D. Y. (2009). "Toxicity assessments of multisized gold and silver nanoparticles in zebrafish embryos." *Small* **5**(16): 1897-1910.

Bastus, N. G., Sanchez-Tillo, E., Pujals, S., Farrera, C., Lopez, C., Giralt, E., et al. (2009). "Homogeneous Conjugation of Peptides onto Gold Nanoparticles Enhances Macrophage Response." *ACS Nano* **3**(6): 1335-1344.

Benedek, T. G. (2004). "The history of gold therapy for tuberculosis." Journal of Historical Medicine and Allied Sciences **59**(1): 50-89

Berry, C. C., de la Fuente, J. M., Mullin, M., Chu, S. W. and Curtis, A. S. (2007). "Nuclear localization of HIV-1 tat functionalized gold nanoparticles." *IEEE Transactions on NanoBioscience* **6**(4): 262-269.

Bhattacharya, R. and Mukherjee, P. (2008). "Biological properties of "naked" metal nanoparticles." *Advanced Drug Delivery Reviews* **60**(11): 1289-1306.

Bohnsack, J. P., Assemi, S., Miller, J. D. and Furgeson, D. Y. (2012). "The primacy of physicochemical characterization of nanomaterials for reliable toxicity assessment: A review of the zebrafish nanotoxicology model." *Methods in Molecular Biology* **926:** 261-316.

Braunbeck, T., Kais, B., Lammer, E., Otte, J., Schneider, K., Stengel, D., et al. (2014). "The fish embryo test (FET): origin, applications, and future." *Environonmental Science and Pollution Research International*: 1-15

Browning, L. M., Huang, T. and Xu, X. H. (2013). "Real-time in vivo imaging of size-dependent transport and toxicity of gold nanoparticles in zebrafish embryos using single nanoparticle plasmonic spectroscopy." *Interface Focus* **3**(3): 20120098.

Browning, L. M., Lee, K. J., Huang, T., Nallathamby, P. D., Lowman, J. E. and Xu, X. H. N. (2009). "Random walk of single gold nanoparticles in zebrafish embryos leading to stochastic toxic effects on embryonic developments." *Nanoscale* **1**(1): 138-152.

Brudal, E., Ulanova, L. S., Lampe, E. O., Rishovd, A. L., Griffiths, G. and Winther-Larsen, H. C. (2014). "Establishment of three Francisella infections in zebrafish embryos at different temperatures." *Infection and Immunity* **82**(6): 2180-2194

Brudal, E., Winther-Larsen, H. C., Colquhoun, D. J. and Duodu, S. (2013). "Evaluation of reference genes for reverse transcription quantitative PCR analyses of fish-pathogenic Francisella strains exposed to different growth conditions." *BMC Research Notes* **6**: 76.

Brun, N. R., Lenz, M., Wehrli, B. and Fent, K. (2014). "Comparative effects of zinc oxide nanoparticles and dissolved zinc on zebrafish embryos and eleuthero-embryos: importance of zinc ions." *Science of the Total Environment* **476-477**: 657-666.

Busquet, F., Strecker, R., Rawlings, J. M., Belanger, S. E., Braunbeck, T., Carr, G. J., et al. (2014). "OECD validation study to assess intra- and inter-laboratory reproducibility of the zebrafish embryo toxicity test for acute aquatic toxicity testing." *Regulatory Toxicology and Pharmacology* **69**(3): 496-511.

Bustin, S. A. (2000). "Absolute quantification of mRNA using real-time reverse transcription polymerase chain reaction assays." *Journal of Molecular Endocrinology* **25**(2): 169-193.

Bustin, S. A. (2002). "Quantification of mRNA using real-time reverse transcription PCR (RT-PCR): trends and problems." *Journal of Molecular Endocrinology* **29**(1): 23-39.

Buzea, C., Pacheco, I. I. and Robbie, K. (2007). "Nanomaterials and nanoparticles: Sources and toxicity." *Biointerphases* **2**(4): 17-71.

Chen, Y.-S., Hung, Y.-C., Liau, I. and Huang, G. S. (2009). "Assessment of the In Vivo Toxicity of Gold Nanoparticles." *Nanoscale Research Letters* **4**(8): 858-864.

Cheng, J. P., Chan, C. M., Veca, L. M., Poon, W. L., Chan, P. K., Qu, L. W., et al. (2009). "Acute and long-term effects after single loading of functionalized multi-walled carbon nanotubes into zebrafish (Danio rerio)." *Toxicology and Applied Pharmacology* **235**(2): 216-225.

Chithrani, B. D., Ghazani, A. A. and Chan, W. C. W. (2006). "Determining the Size and Shape Dependence of Gold Nanoparticle Uptake into Mammalian Cells." *Nano Letters* **6**(4): 662-668.

Cho, W.-S., Cho, M., Jeong, J., Choi, M., Cho, H.-Y., Han, B. S., et al. (2009). "Acute toxicity and pharmacokinetics of 13 nm-sized PEG-coated gold nanoparticles." *Toxicology and Applied Pharmacology* **236**(1): 16-24.

Clemente, Z., Castro, V. L., Moura, M. A., Jonsson, C. M. and Fraceto, L. F. (2014). "Toxicity assessment of TiO nanoparticles in zebrafish embryos under different exposure conditions." *Aquatic Toxicology* **147c**: 129-139.

Commins, S. P., Borish, L. and Steinke, J. W. (2010). "Immunologic messenger molecules: cytokines, interferons, and chemokines." *Journal of Allergy Clinical Immunology* **125**: S53-72.

Croteau, M. N., Dybowska, A. D., Luoma, S. N. and Valsami-Jones, E. (2011). "A novel approach reveals that zinc oxide nanoparticles are bioavailable and toxic after dietary exposures." *Nanotoxicology* **5**(1): 79-90.

Daniel, M. C. and Astruc, D. (2004). "Gold nanoparticles: Assembly, supramolecular chemistry, quantum-size-related properties, and applications toward biology, catalysis, and nanotechnology." *Chemical Reviews* **104**(1): 293-346.

De Jong, W. H., Hagens, W. I., Krystek, P., Burger, M. C., Sips, A. J. A. M. and Geertsma, R. E. (2008). "Particle size-dependent organ distribution of gold nanoparticles after intravenous administration." *Biomaterials* **29**(12): 1912-1919.

de Oliveira, S., Reyes-Aldasoro, C. C., Candel, S., Renshaw, S. A., Mulero, V. and Calado, A. (2013). "Cxcl8 (IL-8) mediates neutrophil recruitment and behavior in the zebrafish inflammatory response." *Journal of Immunology* **190**(8): 4349-4359.

Dobrovolskaia, M. A., Patri, A. K., Zheng, J., Clogston, J. D., Ayub, N., Aggarwal, P., et al. (2009). "Interaction of colloidal gold nanoparticles with human blood: effects on particle size and analysis of plasma protein binding profiles." *Nanomedicine* **5**(2): 106-117.

Donaldson, K., Stone, V., Tran, C. L., Kreyling, W. and Borm, P. J. (2004). "Nanotoxicology." *Occupational and Environ Medicine* **61**(9): 727-728.

Dreaden, E. C., Alkilany, A. M., Huang, X., Murphy, C. J. and El-Sayed, M. A. (2012). "The golden age: gold nanoparticles for biomedicine." *Chemical Society Reviews* **41**(7): 2740-2779.

Driever, W., Solnica-Krezel, L., Schier, A. F., Neuhauss, S. C., Malicki, J., Stemple, D. L., et al. (1996). "A genetic screen for mutations affecting embryogenesis in zebrafish." *Development* **123**: 37-46.

Du, S., Kendall, K., Tolueinia, P., Mehrabadi, Y., Gupta, G. and Newton, J. (2012). "Aggregation and adhesion of gold nanoparticles in phosphate buffered saline." *Journal of Nanoparticle Research* **14**(3): 1-14

Elsabahy, M. and Wooley, K. L. (2013). "Cytokines as biomarkers of nanoparticle immunotoxicity." *Chemical Society Reviews* **42**(12): 5552-5576.

Engeszer, R. E., Patterson, L. B., Rao, A. A. and Parichy, D. M. (2007). "Zebrafish in the Wild: A Review of Natural History and New Notes from the Field." *Zebrafish* **4**(1): 21-U126.

Fako, V. E. and Furgeson, D. Y. (2009). "Zebrafish as a correlative and predictive model for assessing biomaterial nanotoxicity." *Advanced Drug Deliviry Reviews* **61**(6): 478-486.

Filipe, V., Hawe, A. and Jiskoot, W. (2010). "Critical Evaluation of Nanoparticle Tracking Analysis (NTA) by NanoSight for the Measurement of Nanoparticles and Protein Aggregates." *Pharmaceutical Research* **27**(5): 796-810.

Frens, G. (1973). "Controlled Nucleation for the Regulation of the Particle Size in Monodisperse Gold Suspensions." *Nature Physical Science* **241**: 20-22.

Fubini, B., Ghiazza, M. and Fenoglio, I. (2010). "Physico-chemical features of engineered nanoparticles relevant to their toxicity." *Nanotoxicology* **4**: 347-363.

Geffroy, B., Ladhar, C., Cambier, S., Treguer-Delapierre, M., Brethes, D. and Bourdineaud, J. P. (2012). "Impact of dietary gold nanoparticles in zebrafish at very low contamination pressure: The role of size, concentration and exposure time." *Nanotoxicology* **6**(2): 144-160.

Geiser, M., Rothen-Rutishauser, B., Kapp, N., Schurch, S., Kreyling, W., Schulz, H., et al. (2005). "Ultrafine particles cross cellular membranes by nonphagocytic mechanisms in lungs and in cultured cells." *Environmental Health Perspectives* **113**(11): 1555-1560.

Giulietti, A., Overbergh, L., Valckx, D., Decallonne, B., Bouillon, R. and Mathieu, C. (2001). "An overview of real-time quantitative PCR: Applications to quantify cytokine gene expression." *Methods* **25**(4): 386-401.

Goodman, C. M., McCusker, C. D., Yilmaz, T. and Rotello, V. M. (2004). "Toxicity of gold nanoparticles functionalized with cationic and anionic side chains." *Bioconjugate Chemistry* **15**(4): 897-900.

Haffter, P., Granato, M., Brand, M., Mullins, M. C., Hammerschmidt, M., Kane, D. A., et al. (1996). "The identification of genes with unique and essential functions in the development of the zebrafish, Danio rerio." *Development* **123**: 1-36.

Hamilton, F. (1822). An account of the fishes found in the river Ganges and its branches (Online) Accessed: 29.04.15 from https://archive.org/details/accountoffishesf00hami

Harper, S., Usenko, C., Hutchison, J. E., Maddux, B. L. S. and Tanguay, R. L. (2008). "In vivo biodistribution and toxicity depends on nanomaterial composition, size, surface functionalisation and route of exposure." *Journal of Experimental Nanoscience* **3**(3): 195-206.

He, X., Young, S. H., Schwegler-Berry, D., Chisholm, W. P., Fernback, J. E. and Ma, Q. (2011). "Multiwalled carbon nanotubes induce a fibrogenic response by stimulating reactive oxygen species production, activating NF-kappaB signaling, and promoting fibroblast-to-myofibroblast transformation." *Chemical Research of Toxicology* **24**(12): 2237-2248.

Herbomel, P., Thisse, B. and Thisse, C. (1999). "Ontogeny and behaviour of early macrophages in the zebrafish embryo." *Development* **126**(17): 3735-3745.

Hillyer, J. F. and Albrecht, R. M. (2001). "Gastrointestinal persorption and tissue distribution of differently sized colloidal gold nanoparticles." *Journal Pharmaceutical Science* **90**(12): 1927-1936.

Hirsch, L. R., Stafford, R. J., Bankson, J. A., Sershen, S. R., Rivera, B., Price, R. E., et al. (2003). "Nanoshell-mediated near-infrared thermal therapy of tumors under magnetic resonance guidance." *Proceedings of the National Academy of Sciences of the United States of America* **100**(23): 13549-13554.

Hornyak, G. L., Moore, J. J., Ibbals, H.F and Dutta, J. (2009). Fundamentals of nanotechnology. Boca Raton, Fl, CRC Press.

Howe, K., Clark, M. D., Torroja, C. F., Torrance, J., Berthelot, C., Muffato, M., et al. (2013). "The zebrafish reference genome sequence and its relationship to the human genome." *Nature* **496**(7446): 498-503.

Huang, X. H., El-Sayed, I. H., Qian, W. and El-Sayed, M. A. (2006). "Cancer cell imaging and photothermal therapy in the near-infrared region by using gold nanorods." *Journal of the American Chemical Society* **128**(6): 2115-2120.

Hurst, S. J. (2011). "Biomedical nanotechnology." *Methods in Molecular Biology* **726**: 1-13.

Hussain, S. M., Hess, K. L., Gearhart, J. M., Geiss, K. T. and Schlager, J. J. (2005). "In vitro toxicity of nanoparticles in BRL 3A rat liver cells." *Toxicology in Vitro* **19**(7): 975-983.

Ito, K., Takizawa, F., Yoshiura, Y., Ototake, M. and Nakanishi, T. (2008). "Expression profile of cytokine and transcription factor genes during embryonic development of zebrafish Danio rerio." *Fisheries Science* **74**(2): 391-396.

Jin, Y., Liu, Z., Liu, F., Ye, Y., Peng, T. and Fu, Z. (2015). "Embryonic exposure to cadmium (II) and chromium (VI) induce behavioral alterations, oxidative stress and immunotoxicity in zebrafish (Danio rerio)." *Neurotoxicology and Teratology* **48**: 9-17.

Jovanović, B., Ji, T. and Palić, D. (2011). "Gene expression of zebrafish embryos exposed to titanium dioxide nanoparticles and hydroxylated fullerenes." *Ecotoxicology and Environmental Safety* **74**(6): 1518-1525.

Kamat, P. V. (2002). "Photophysical, photochemical and photocatalytic aspects of metal nanoparticles." *Journal of Physical Chemistry B* **106**(32): 7729-7744.

Karlsson, H. L., Cronholm, P., Gustafsson, J. and Moeller, L. (2008). "Copper oxide nanoparticles are highly toxic: A comparison between metal oxide nanoparticles and carbon nanotubes." *Chemical Research in Toxicology* **21**(9): 1726-1732.

Kelly, K. L., Coronado, E., Zhao, L. L. and Schatz, G. C. (2003). "The optical properties of metal nanoparticles: The influence of size, shape, and dielectric environment." *Journal of Physical Chemistry B* **107**(3): 668-677.

Kessler, R. (2011). "Engineered nanoparticles in consumer products: understanding a new ingredient." *Environmental Health Perspective* **119**(3): a120-125.

Kettiger, H., Schipanski, A., Wick, P. and Huwyler, J. (2013). "Engineered nanomaterial uptake and tissue distribution: from cell to organism." *International Journal of Nanomedicine* **8**: 3255-3269.

Khan, H. A., Abdelhalim, M. A., Alhomida, A. S. and Al Ayed, M. S. (2013). "Transient increase in IL-1beta, IL-6 and TNF-alpha gene expression in rat liver exposed to gold nanoparticles." *Genetics and Molecular Research* **12**(4): 5851-5857.

Khan, M. S., Vishakante, G. D. and Siddaramaiah, H. (2013). "Gold nanoparticles: a paradigm shift in biomedical applications." *Advances in Colloid and Interface Science* **199-200**: 44-58.

Khlebtsov, N. and Dykman, L. (2011). "Biodistribution and toxicity of engineered gold nanoparticles: a review of in vitro and in vivo studies." *Chemical Society Reviews* **40**(3): 1647-1671.

Kim, K. T., Zaikova, T., Hutchison, J. E. and Tanguay, R. L. (2013). "Gold Nanoparticles Disrupt Zebrafish Eye Development and Pigmentation." *Toxicological Sciences* **133**(2): 275-288.

Kim, S., Choi, J. E., Choi, J., Chung, K.-H., Park, K., Yi, J., et al. (2009). "Oxidative stress-dependent toxicity of silver nanoparticles in human hepatoma cells." *Toxicology in Vitro* **23**(6): 1076-1084.

Kimling, J., Maier, M., Okenve, B., Kotaidis, V., Ballot, H. and Plech, A. (2006). "Turkevich method for gold nanoparticle synthesis revisited." *Journal of Physical Chemistry B* **110**(32): 15700-15707.

Kimmel, C. B., Ballard, W. W., Kimmel, S. R., Ullmann, B. and Schilling, T. F. (1995). "Stages of embryonic development of the zebrafish." *Developmental Dynamics* **203**(3): 253-310.

Kimmel, C. B., Warga, R. M. and Schilling, T. F. (1990). "Origin and organization of the zebrafish fate map." *Development* **108**(4): 581-594.

King-Heiden, T. C., Mehta, V., Xiong, K. M., Lanham, K. A., Antkiewicz, D. S., Ganser, A., et al. (2012). "Reproductive and developmental toxicity of dioxin in fish." *Molecular and Cellular Endocrinology* **354**(1-2): 121-138.

Kirpotin, D. B., Drummond, D. C., Shao, Y., Shalaby, M. R., Hong, K., Nielsen, U. B., et al. (2006). "Antibody targeting of long-circulating lipidic nanoparticles does not increase tumor localization but does increase internalization in animal models." *Cancer Research* **66**(13): 6732-6740.

Klaasen, D. C. (2001). Casarett and Doull´s Toxicology: The Basic Science of Poisons. USA, McGraw- Hill.

Kovriznych, J. A., Sotnikova, R., Zeljenkova, D., Rollerova, E., Szabova, E. and Wimmerova, S. (2013). "Acute toxicity of 31 different nanoparticles to zebrafish (Danio rerio) tested in adulthood and in early life stages - comparative study." *Interdisciplinary Toxicology* **6**(2): 67-73.

Lam, S. H., Chua, H. L., Gong, Z., Lam, T. J. and Sin, Y. M. (2004). "Development and maturation of the immune system in zebrafish, Danio rerio: a gene expression profiling, in situ hybridization and immunological study." *Developmental and Comparative Immunology* **28**(1): 9-28.

Lee, K. S. and El-Sayed, M. A. (2006). "Gold and silver nanoparticles in sensing and imaging: sensitivity of plasmon response to size, shape, and metal composition." *Journal of Physical Chemistry B* **110**(39): 19220-19225.

Lee, Y. K., Choi, E. J., Webster, T. J., Kim, S. H. and Khang, D. (2015). "Effect of the protein corona on nanoparticles for modulating cytotoxicity and immunotoxicity." *International Journal of Nanomedicine* **10**: 97-113.

Li, J. J., Hartono, D., Ong, C.-N., Bay, B.-H. and Yung, L.-Y. L. (2010). "Autophagy and oxidative stress associated with gold nanoparticles." *Biomaterials* **31**(23): 5996-6003.

Licastro, F., Candore, G., Lio, D., Porcellini, E., Colonna-Romano, G., Franceschi, C., et al. (2005). "Innate immunity and inflammation in ageing: a key for understanding age-related diseases." *Immunity and Ageing* **2**: 8.

Liu, X., Huang, N., Li, H., Jin, Q. and Ji, J. (2013). "Surface and size effects on cell interaction of gold nanoparticles with both phagocytic and nonphagocytic cells." *Langmuir* **29**(29): 9138-9148.

McCurley, A. T. and Callard, G. V. (2008). "Characterization of housekeeping genes in zebrafish: male-female differences and effects of tissue type, developmental stage and chemical treatment." *BMC Molecular Biology* **9**: 102.

Mogensen, T. H. (2009). "Pathogen recognition and inflammatory signaling in innate immune defenses." *Clinical and Microbiology Reviews* **22**(2): 240-273.

Monopoli, M. P., Walczyk, D., Campbell, A., Elia, G., Lynch, I., Bombelli, F. B., et al. (2011). "Physical-chemical aspects of protein corona: relevance to in vitro and in vivo biological impacts of nanoparticles." *Journal of the American Chemical Society* **133**(8): 2525-2534.

Murdock, R. C., Braydich-Stolle, L., Schrand, A. M., Schlager, J. J. and Hussain, S. M. (2008). "Characterization of nanomaterial dispersion in solution prior to in vitro exposure using dynamic light scattering technique." *Toxicological Sciences* **101**(2): 239-253.

Oberdorster, G., Maynard, A., Donaldson, K., Castranova, V., Fitzpatrick, J., Ausman, K., et al. (2005b). "Principles for characterizing the potential human health effects from exposure to nanomaterials: elements of a screening strategy." *Particle and fibre toxicology* **2**: 8-8.

Oberdorster, G., Oberdorster, E. and Oberdorster, J. (2005a). "Nanotoxicology: an emerging discipline evolving from studies of ultrafine particles." *Environmental Health Perspectives* **113**(7): 823-839.

Opal, S. M. and DePalo, V. A. (2000). "Anti-inflammatory cytokines." *Chest* **117**(4): 1162-1172.

Owens, D. E., 3rd and Peppas, N. A. (2006). "Opsonization, biodistribution, and pharmacokinetics of polymeric nanoparticles." *International Journal of Pharmaceuticals* **307**(1): 93-102.

Paciotti, G. F., Myer, L., Weinreich, D., Goia, D., Pavel, N., McLaughlin, R. E., et al. (2004). "Colloidal gold: A novel nanoparticle vector for tumor directed drug delivery." *Drug Delivery* **11**(3): 169-183.

Pan, Y., Leifert, A., Ruau, D., Neuss, S., Bornemann, J., Schmid, G., et al. (2009). "Gold nanoparticles of diameter 1.4 nm trigger necrosis by oxidative stress and mitochondrial damage." *Small* **5**(18): 2067-2076.

Park, J. W., Henry, T. B., Menn, F. M., Compton, R. N. and Sayler, G. (2010). "No bioavailability of 17alpha-ethinylestradiol when associated with nC60 aggregates during dietary exposure in adult male zebrafish (Danio rerio)." *Chemosphere* **81**(10): 1227-1232.

Piccinno, F., Gottschalk, F., Seeger, S. and Nowack, B. (2012). "Industrial production quantities and uses of ten engineered nanomaterials in Europe and the world." *Journal of Nanoparticle Research* **14**(9).

Powers, K. W., Palazuelos, B. M. and Roberts, S. M. (2007). "Characterization of the size, shape, and state of dispersion of nanoparticles for toxicological studies." Nanotoxicology **1**: 42-51.

Roca, F. J., Mulero, I., Lopez-Munoz, A., Sepulcre, M. P., Renshaw, S. A., Meseguer, J., et al. (2008). "Evolution of the inflammatory response in vertebrates: fish TNF-alpha is a powerful activator of endothelial cells but hardly activates phagocytes." J Immunol **181**(7): 5071-5081.

Roco, M. C. (2005b). "International Perspective on Government Nanotechnology Funding in 2005." *Journal of Nanoparticle Research* **7**(6): 707-712.

Roco, M. C. and Bainbridge, W. S. (2005a). "Societal implications of nanoscience and nanotechnology: Maximizing human benefit." *Journal of Nanoparticle Research* **7**(1): 1-13.

Rojo, I., de Ilarduya, O. M., Estonba, A. and Pardo, M. A. (2007). "Innate immune gene expression in individual zebrafish after Listonella anguillarum inoculation." *Fish Shellfish Immunology* **23**(6): 1285-1293.

Rubinstein, A. L. (2006). "Zebrafish assays for drug toxicity screening." *Expert Opinion on Drug Metabolism and Toxicology* **2**(2): 231-240.

Schaeublin, N. M., Braydich-Stolle, L. K., Schrand, A. M., Miller, J. M., Hutchison, J., Schlager, J. J., et al. (2011). "Surface charge of gold nanoparticles mediates mechanism of toxicity." *Nanoscale* **3**(2): 410-420.

Selderslaghs, I. W., Van Rompay, A. R., De Coen, W. and Witters, H. E. (2009). "Development of a screening assay to identify teratogenic and embryotoxic chemicals using the zebrafish embryo." *Reproductive Toxicology* **28**(3): 308-320.

Seppola, M., Larsen, A. N., Steiro, K., Robertsen, B. and Jensen, I. (2008). "Characterisation and expression analysis of the interleukin genes, IL-1beta, IL-8 and IL-10, in Atlantic cod (Gadus morhua L.)." *Molecular Immunology* **45**(4): 887-897.

Sharma, M., Salisbury, R. L., Maurer, E. I., Hussain, S. M. and Sulentic, C. E. (2013). "Gold nanoparticles induce transcriptional activity of NF-kappaB in a B-lymphocyte cell line." *Nanoscale* **5**(9): 3747-3756.

Shin, Y. J., Nam, S. H. and An, Y. J. (2014). "Japanese medaka exposed to gold nanoparticles: Only embryonic exposure generates irreversible hatching failure, developmental failure, and mortality of sac-fry." *Comparative Biochemisty and Physiology - Part C* **161**: 26-32.

Shukla, R., Bansal, V., Chaudhary, M., Basu, A., Bhonde, R. R. and Sastry, M. (2005). "Biocompatibility of gold nanoparticles and their endocytotic fate inside the cellular compartment: a microscopic overview." *Langmuir* **21**(23): 10644-10654.

Sieger, D., Stein, C., Neifer, D., van der Sar, A. M. and Leptin, M. (2009). "The role of gamma interferon in innate immunity in the zebrafish embryo." *Disease Model and Mechanisms* **2**(11-12): 571-581.

Sigler, J. W., et al. (1974). "Gold salts in the treatment of rheumatoid arthritis. A double-blind study." Annual International Medicine **80**(1): 21-26.

Simpson, C. A., Huffman, B. J., Gerdon, A. E. and Cliffel, D. E. (2010). "Unexpected toxicity of monolayer protected gold clusters eliminated by PEG-thiol place exchange reactions." *Chemical Research and Toxicology* **23**(10): 1608-1616.

Sipes, N. S., Padilla, S. and Knudsen, T. B. (2011). "Zebrafish: as an integrative model for twenty-first century toxicity testing." *Birth Defects Research Part C: Embryo Today* **93**(3): 256-267.

Sohaebuddin, S. K., Thevenot, P. T., Baker, D., Eaton, J. W. and Tang, L. (2010). "Nanomaterial cytotoxicity is composition, size, and cell type dependent." *Particle and Fibre Toxicology* **7**:22.

Stein, C., Caccamo, M., Laird, G. and Leptin, M. (2007). "Conservation and divergence of gene families encoding components of innate immune response systems in zebrafish." *Genome Biology* **8**(11): R251.

Storm, G., Belliot, S. O., Daemen, T. and Lasic, D. D. (1995). "Surface modification of nanoparticles to oppose uptake by the mononuclear phagocyte system." *Advanced Drug Delivery Reviews* **17**(1): 31-48.

Tang, R., Dodd, A., Lai, D., McNabb, W. C. and Love, D. R. (2007). "Validation of zebrafish (Danio rerio) reference genes for quantitative real-time RT-PCR normalization." *Acta Biochimica et Biophysica Sinica* **39**(5): 384-390.

Taylor, K. L., Grant, N. J., Temperley, N. D. and Patton, E. E. (2010). "Small molecule screening in zebrafish: an in vivo approach to identifying new chemical tools and drug leads." *Cell Communication and Signaling* **8**: 11.

Tedesco, S., Doyle, H., Blasco, J., Redmond, G. and Sheehan, D. (2010). "Oxidative stress and toxicity of gold nanoparticles in Mytilus edulis." *Aquatic Toxicology* **100**(2): 178-186.

Thannickal, V. J. and Fanburg, B. L. (2000). "Reactive oxygen species in cell signaling." *American Journal of Physiology Lung Cellular and Molecular Physiology* **279**(6): L1005-1028.

Traver, D., Herbomel, P., Patton, E. E., Murphey, R. D., Yoder, J. A., Litman, G. W., et al. (2003). "The zebrafish as a model organism to study development of the immune system." *Advances in Immunology* **1**: 253-330

Trede, N. S., Langenau, D. M., Traver, D., Look, A. T. and Zon, L. I. (2004). "The Use of Zebrafish to Understand Immunity." *Immunity* **20**(4): 367-379.

Truong, L., Saili, K. S., Miller, J. M., Hutchison, J. E. and Tanguay, R. L. (2012). "Persistent adult zebrafish behavioral deficits results from acute embryonic exposure to gold nanoparticles." *Comparative Biochemistry and Physiology C-Toxicology & Pharmacology* **155**(2): 269-274.

Truong, L., Tilton, S. C., Zaikova, T., Richman, E., Waters, K. M., Hutchison, J. E., et al. (2013). "Surface functionalities of gold nanoparticles impact embryonic gene expression responses." *Nanotoxicology* **7**(2): 192-201.

Turkevich, J., Stevenson, P. C. and Hillier, J. (1951). "A study of the nucleation and growth processes in the synthesis of colloidal gold." *Discussions of the Faraday Society* **11**: 55-75.

van der Vaart, M., Spaink, H. P. and Meijer, A. H. (2012). "Pathogen recognition and activation of the innate immune response in zebrafish." *Advanced Hematology* **2012**: 159807.

Vandesompele, J., De Preter, K., Pattyn, F., Poppe, B., Van Roy, N., De Paepe, A., et al. (2002). "Accurate normalization of real-time quantitative RT-PCR data by geometric averaging of multiple internal control genes." *Genome Biology* **3**(7): Research0034.

Walkey, C. D., Olsen, J. B., Guo, H., Emili, A. and Chan, W. C. W. (2012). "Nanoparticle Size and Surface Chemistry Determine Serum Protein Adsorption and Macrophage Uptake." *Journal of the American Chemical Society* **134**(4): 2139-2147.

Wang, J., Liu, Y., Jiao, F., Lao, F., Li, W., Gu, Y., et al. (2008). "Time-dependent translocation and potential impairment on central nervous system by intranasally instilled TiO2 nanoparticles." *Toxicology* **254**(1-2): 82-90.

Wang, Y. L., Seebald, J. L., Szeto, D. P. and Irudayaraj, J. (2010). "Biocompatibility and Biodistribution of Surface-Enhanced Raman Scattering Nanoprobes in Zebrafish Embryos: In vivo and Multiplex Imaging." *Acs Nano* **4**(7): 4039-4053.

Westerfield, M. (2000). The zebrafish book: A guide for the laboratory use of zebrafish (Danio rerio). Eugene, Univ. of Oregon Press.

Xia, T., Kovochich, M., Liong, M., Maedler, L., Gilbert, B., Shi, H., et al. (2008). "Comparison of the Mechanism of Toxicity of Zinc Oxide and Cerium Oxide Nanoparticles Based on Dissolution and Oxidative Stress Properties." *Acs Nano* **2**(10): 2121-2134.
Yan, J., Lin, B., Hu, H., Zhang., H., Lin, Z., Zhuge, X. (2014). "The combined toxicological effect of titanium dioxide nanoparticles and bisphenol A on zebrafish embryos." *Nanoscale Research Letters* **9**(1): 406

Yen, H. J., Hsu, S. H. and Tsai, C. L. (2009). "Cytotoxicity and Immunological Response of Gold and Silver Nanoparticles of Different Sizes." *Small* **5**(13): 1553-1561.

Yeo, M. K. and Kim, H. E. (2010). "Gene expression in zebrafish embryos following exposure to TiO2 nanoparticles." *Molecular and Cellular Toxicology* **6**(1): 97-104.

Zhang, C., Willett, C. and Fremgen, T. (2003). "Zebrafish: an animal model for toxicological studies." *Current Protocol in Toxicology* **Chapter 1**: Unit1.7.

Zhang, D. C., Shao, Y. Q., Huang, Y. Q. and Jiang, S. G. (2005). "Cloning, characterization and expression analysis of interleukin-10 from the zebrafish (Danio rerion)." *Journal of Biochemistry and Molecular Biology* **38**(5): 571-576.

Zon, L. I. and Peterson, R. T. (2005). "In vivo drug discovery in the zebrafish." *Nature Reviews Drug Discovery* **4**(1): 35-44.

Appendix A: Kit protocols

A.1 RNeasy Mini Kit (QIAGEN): Purification of Total RNA from Animal Tissues

1-3. Disruption and homogenization of animal tissue

4. Centrifuge the lysate for 3 min at full speed. Carefully remove the supernatant by pipetting and transfer it to a new microcentrifuge tube (not supplied). Use only this supernatant (lysate) in subsequent steps. In some preparations very small amounts of insoluble material will be present after the 3 min centrifugation making the pellet invisible.

5. Add 1 volume of 70% ethanol to the cleared lysate and mix immediately by pipetting. Do not centrifuge. Proceed immediately to step 6.

Note: The volume of lysate may be less than 350 or 600µl due to loss during homogenization and centrifugation in steps 3 and 4.

Note: Precipitates may be visible after addition of ethanol. This does not affect the procedure.

6. Transfer up to 700 µl of the sample including any precipitate that may have formed to an RNeasy spin column placed in a 2 ml collection tube (supplied). Close the lid gently and centrifuge for 15 s at ≥8000 x g (≥10.000 rpm). Discard the flow-through.
Reuse the collection tube in step 7.
If the sample volume exceeds 700 µl. centrifuge successive aliquots in the same RNeasy spin column. Discard the flow-through after each centrifugation.

Optional step: DNase treatment

D1. Add 350 µl Buffer RW1 to the RNeasy spin column. Close the lid gently. and centrifuge for 15 s at ≥8000 x g (≥10.000 rpm) to wash the spin column membrane.
Discard the flow-through.
Reuse the collection tube in step D4.
D2. Add 10 µl DNase I stock solution (see above) to 70 µl Buffer RDD. Mix by gently inverting the tube and centrifuge briefly to collect residual liquid from the sides.
Buffer RDD is supplied with the RNase-Free DNase Set.

Note: DNase is especially sensitive to physical denaturation. Mixing should only be carried out by gently inverting the tube. Do not vortex.
D3. Add the DNase I incubation mix (80 µl) directly to the RNeasy spin column membrane and place on the benchtop (20-30° C) for 15 min.
Note: Be sure to add the DNase I incubation mix directly to the RNeasy spin column membrane. DNase digestion will be incomplete if part of the mix sticks to the walls or the O-ring of the spin column.
D4. Add 350 µl Buffer RW1 to the RNeasy spin column. Close the lid gently and centrifuge for 15 s at ≥8000 x g (≥10.000 rpm) Discard the flow-through.
Continue with the first Buffer RPE wash step in the relevant protocol.

Note: In most of the protocols the immediately following Buffer RW1 wash step is skipped (as indicated in the protocol). Continue with the first Buffer RPE wash step.

8. Add 500 µl Buffer RPE to the RNeasy spin column. Close the lid gently. and centrifuge for 15 s at ≥8000 x g (≥10.000 rpm) to wash the spin column membrane.
Discard the flow-through.
Reuse the collection tube in step 9.
Note: Buffer RPE is supplied as a concentrate. Ensure that ethanol is added to Buffer RPE before use.

9. Add 500 µl Buffer RPE to the RNeasy spin column. Close the lid gently and centrifuge for 2min at ≥8000 x g (≥10.000 rpm) to wash the spin column membrane.

The long centrifugation dries the spin column membrane ensuring that no ethanol is carried over during RNA elution. Residual ethanol may interfere with downstream reactions.

Note: After centrifugation, carefully remove the RNeasy spin column from the collection tube so that the column does not contact the flow-through. Otherwise carryover of ethanol will occur.

10. Optional: Place the RNeasy spin column in a new 2 ml collection tube (supplied), and discard the old collection tube with the flow-through. Close the lid gently, and centrifuge at full speed for 1 min.
Perform this step to eliminate any possible carryover of Buffer RPE, or if residual flow-through remains on the outside of the RNeasy spin column after step 9.

11. Place the RNeasy spin column in a new 1.5 ml collection tube (supplied). Add 30-50 µl RNase-free water directly to the spin column membrane. Close the lid gently and centrifuge for 1 min at ≥8000 x g (≥10.000 rpm) to elute the RNA.

A.2 High Capacity RNA-to-cDNA Kit (Applied Biosystems)

1. Use up to 2 μg of total RNA per 20 μL reaction.
2. Allow kit components to thaw on ice.
3. Referring to the table below, calculate the volume of components needed to prepare the required number of reactions.
4. Aliquot RT reaction mix into plates or tubes.
5. Seal the tubes with appropriate caps.
6. Place the tubes on ice until you are ready to start the reverse transcription reactions
7. Incubate the reaction for 37° C for 60 minutes. Stop the reactions by heating to 95° C for 5 minutes and hold at 4° C. For convenience the incubation may be performed in a thermal cycler.
8. The cDNA is ready for use in a real-time PCR application or long-term storage in freezer (-15° C to -20° C).

Component	**Component Volume/Reaction (μL)**	
	+RT reaction	- RT reaction
2X RT Buffer	10.0	10.0
20X Enzyme Mix	1.0	-
RNA Sample	up to 9 μL	up to 9 μL
Nuclease-free H2O	Q.S.* to 20 μL	Q.S.* to 20 μL
Total per Reaction	20.0	20.0

* Quantity Sufficient

A.3 Master Mix for qPCR reactions

Component volumes for one RT reaction

Component	**Component Volume/Reaction (μL)**	
Manufacturer	**QIAGEN**	**Invitrogen***
SYBER green	10.0	10
Primers	2.0 (F+R)	2.0 F + 2.0 R
RNase free water	3.0	1.0
Total per reaction	20.0	20.0

* Forward and revers primers from Invitrogen (*18S* and *EF1a*) are provided in separate tubes

Appendix B: Pilot study and other results

B.1 .Pilot Study

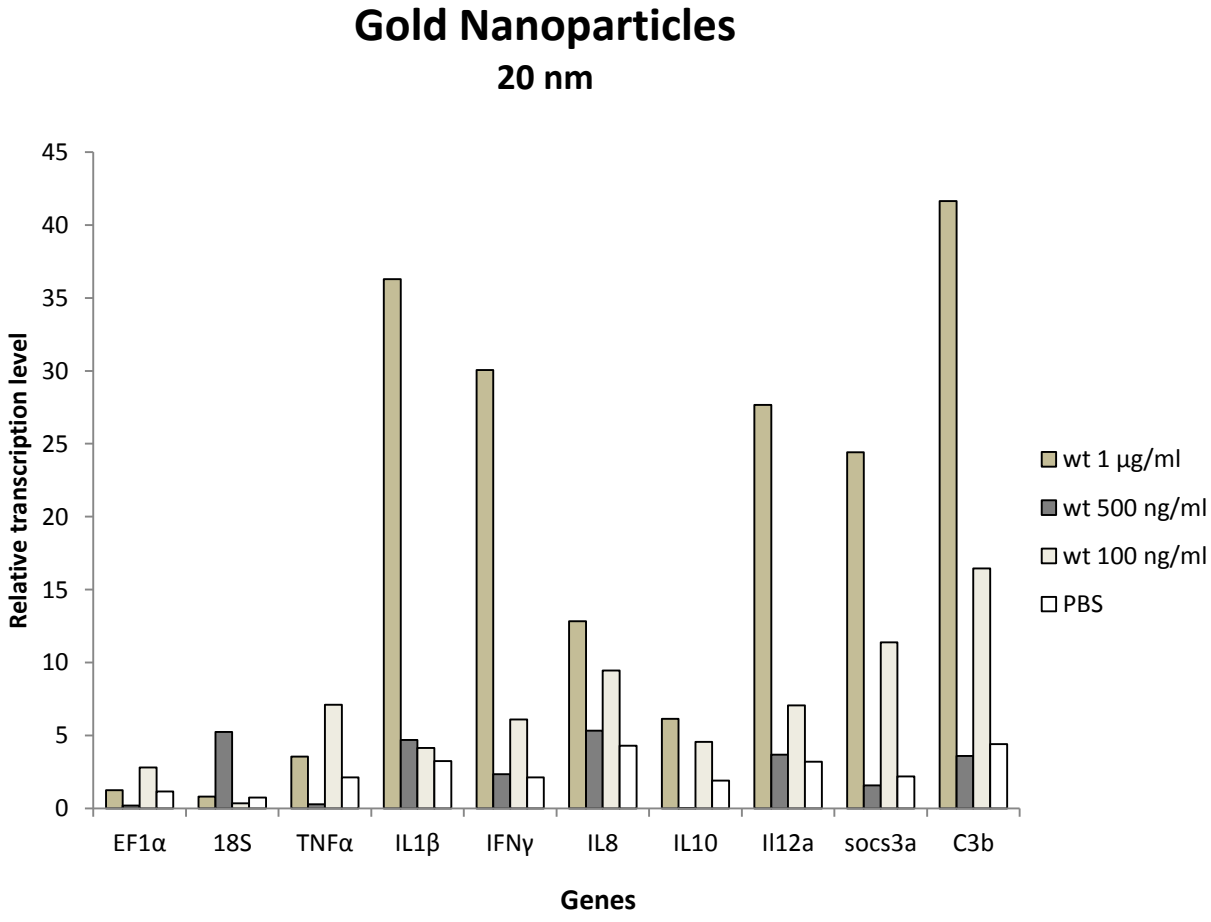

Figure B.1: *Relative transcription levels from the pilot study of the reference genes (EF1a and 18S) and the inflammatory genes (TNFa, IL1b, IL8, IL10, IL12a, socs3a and C3b). Results are from one replicate and consisted of zebrafish embryos injected with 0.1, 0.5 or 1.0 µg/ml of 20 nm gold nanoparticles into the duct of Cuvier at 72 hpf. PBS was used as the solvent contro*

B.2. Relative expression of the reference genes

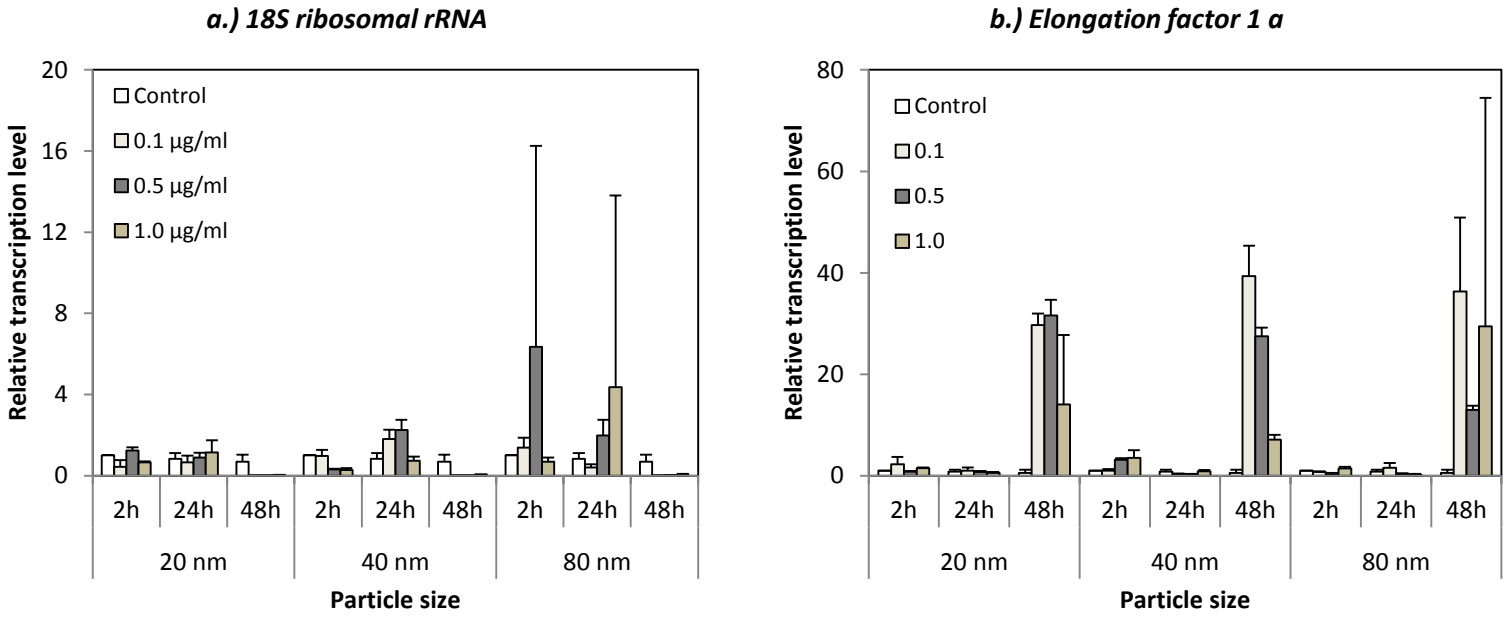

Figure B2: *Relative expression levels at 2, 24 and 48 h = hours post injection of the reference genes that were used to normalize the transcription levels of the immune response. (a) 18S rRNA and (b) EF1a in zebrafish embryos injected with 0.1, 0.5 or 1.0 µg/ml of 20, 40 or 80 nm AuNPs at 72 hpf. Data are presented as the mean ± SEM.*